Heat pump systems for multifamily buildings: Potential and constraints of several heat sources for diverse building demands

De Sousa Fraga, Carolina; Hollmuller, Pierre; Schneider, Stefan; Lachal, Bernard Marie

How to cite

DE SOUSA FRAGA, Carolina et al. Heat pump systems for multifamily buildings: Potential and constraints of several heat sources for diverse building demands. In: Applied Energy, 2018, vol. 225, p. 1033–1053. doi: 10.1016/j.apenergy.2018.05.004

This publication URL: https://archive-ouverte.unige.ch/unige:104908
Publication DOI: 10.1016/j.apenergy.2018.05.004

Heat pump systems for multifamily buildings: potential and constraints of several heat sources for diverse building demands

Carolina Fraga*, Pierre Hollmuller, Stefan Schneider, Bernard Lachal
Energy Systems Group, University of Geneva, Section of Earth and Environmental Sciences, Department F.-A. Forel for environmental and aquatic sciences & Institute for Environmental Sciences
Uni Carl Vogt, 66 boulevard Carl Vogt 1211 Geneva 4, Switzerland
*corresponding author: carolina.fraga@unige.ch, Tel: +41 22 379 01 07

Abstract

This article covers a comparative analysis of the potentials and constraints of different heat sources (air, geothermal boreholes, lake, river, groundwater and solar thermal) exploited by HP systems, implemented in various types of multifamily buildings (MFB) – new, retrofitted and non-retrofitted – which correspond to real case studies situated in Geneva. After characterizing the various heat sources and building demands, as well as presenting the numerical model and adopted sizing values, we study the intrinsic potential of the various HP heat sources and show that the HP seasonal performance factor (SPF) is directly correlated to the heat source temperature. In a further step we consider complementary PV production for the HP system, taking into account the available roof area and daily profile match. For buildings with a combined space heating and domestic hot water heat demand up to 80 kWh/m^2, which correspond to current best case buildings (10% of the existing MFB stock in Geneva), combined HP & PV systems should lead to an annual purchased electricity inferior to 15 kWh/m^2 (with a factor 2 between best and worst heat sources), with an associated daily peak load up to 150 Wh/m^2/day. For a demand below 130 kWh/m^2 (which is the case of 75% of the existing MFB stock of the Canton), the various combinations of HP & PV systems mainly result in a purchased electricity below 45 kWh/m^2. The daily peak load reaches up to 500 Wh/m^2/day, or eventually higher in the case of high-rise buildings. Aside from the final purchased electricity, the annual electricity injected into the grid is in the order of 15 – 20 kWh/m^2 for low-rise buildings, and half that much for high-rise buildings (except for solar HP systems, for which the reduced available roof area for PV leads to significantly lower values). Lastly, SPF alone is not a sufficient indicator for the characterization of the HP system performance, since it doesn't reflect the absolute value of the electricity demand, which primarily depends on the building heat demand. Furthermore, both SPF and annual electricity demand are limited to annual balance considerations. As a complement, an indication of the peak electricity load gives valuable indications of the potential stress on the grid.

Keywords

heat pump (HP), photovoltaic (PV), multifamily building, heat source, electric grid, system performance indicator

Nomenclature

Abbreviations

ASHP	air source heat pump
DHW	domestic hot water
GSHP	ground source heat pump
GWHP	groundwater heat pump
HP	heat pump
SFB	single family building
SHP	solar thermal heat pump
SH	space heating
ST	solar thermal
MFB	multifamily building
PV	photovoltaic

Latin letters

A_{geo}	geothermal footprint per heated area, taking into account surface availability [m^2/m^2]
$A_{geo.0}$	geothermal footprint per heated area, without considering surface availability [m^2/m^2]
A_{sol}	specific solar collector area per heated area, taking into surface availability [m^2/m^2]
$A_{sol.0}$	specific solar collector area per heated area, without considering surface availability [m^2/m^2]
COP	coefficient of performance [-]
E_{app}	electricity, of appliances [kWh/m^2]
$E_{app,pv}$	electricity, of appliances covered by excess PV [kWh/m^2]
E_{dir}	electricity, direct heating [kWh/m^2]
E_{final}	electricity, purchased from the grid [kWh/m^2]
E_{hp}	electricity, HP [kWh/m^2]
E_{inject}	electricity, PV production injected into the grid [kWh/m^2]
E_{pv}	electricity, total PV production [kWh/m^2]
E_{self}	electricity, self-consumed PV production [kWh/m^2]
E_{sys}	electricity, HP + direct heating [kWh/m^2]
$P_{max,dem}$	maximum hourly heat load, DHW + SH [W/m^2]
$P_{max,dhw}$	maximum hourly heat load, DHW [W/m^2]
$P_{max,sh}$	maximum hourly heat load, SH [W/m^2]
$P_{nom,hp}$	nominal capacity, HP [W/m^2]
$P_{nom,sh.0°C}$	nominal heat load, SH (at 0°C outdoor) [W/m^2]
Q_{dem}	heat demand, DHW + SH [kWh/m^2]
Q_{dhw}	heat demand, DHW [kWh/m^2]
Q_{hp}	HP heat production [kWh/m^2]
$Q_{hp,dhw}$	HP heat production, to DHW [kWh/m^2]
$Q_{hp,sh}$	HP heat production, to SH [kWh/m^2]
$Q_{hp,st}$	HP heat production, to storage [kWh/m^2]
$Q_{hs,hp}$	heat from heat source, to HP [kWh/m^2]
Q_{sh}	heat demand, SH [kWh/m^2]
$Q_{sol,dhw}$	direct solar heat production, to DHW [kWh/m^2]
$Q_{sol,dir}$	direct solar heat production, to SH + DHW + storage [kWh/m^2]
$Q_{sol,hp}$	solar collector heat production, to HP [kWh/m^2]
$Q_{sol,sh}$	direct solar heat production, to SH [kWh/m^2]
$Q_{st,dhw}$	storage heat discharge, to DHW [kWh/m^2]
$Q_{st,loss}$	storage heat losses [kWh/m^2]

$Q_{st,sh}$	storage heat discharge, to SH [kWh/m^2]
SPF_{final}	seasonal performance factor, combined HP and PV system [-]
SPF_{hp}	seasonal performance factor, HP only [-]
SPF_{sys}	seasonal performance factor, HP system [-]
St_{hp}	upper DHW storage capacity [L/m^2]
St_{sh}	SH storage capacity [L/m^2]
St_{sol}	lower DHW storage capacity [L/m^2]
$T_{sh.0°C}$	temperature of SH distribution, at 0° outdoor temperature [°C]
$T_{sh.15°C}$	temperature of SH distribution, at 15°C outdoor temperature [°C]
$T_{sh.off}$	temperature on/off set-point for SH, outdoor temperature [°C]

1. Introduction

Over the past decade, heat pumps (HP) have become a key technology for the increased use of renewable energy resources. Nowadays, the most common HP systems are air source (ASHP) or ground source (GSHP) systems. Nevertheless, in view of increasing the system performance, focus has lately been set on combining HPs and solar thermal (ST) collectors, which in turn rises the issue of competition or synergy between ST and photovoltaic (PV). On the other hand, massive HP introduction and the associated increase of electricity demand may have an important impact on the electric grid.

After an overview of existing studies concerning preceding issues, which mainly concern single family buildings (SFB), we introduce the specific issues concerning HP systems in multifamily buildings (MFB). Within this general framework, we then present the specific context and objectives of our work.

HP performance indicators

One of the major issues concerning the use of HPs is their associated electricity consumption. The performance of HP systems is therefore commonly quantified: i) at the level of the HP by the COP and SPF_{hp}, both defined as the ratio between the heat produced by the HP and the electricity consumed by the HP, COP concerning instantaneous values whereas SPF_{hp} annual values; ii) at the level of the heating system by the SPF_{sys}, defined as the ratio between total system heat production and related electricity consumption, including auxiliary electricity. Several projects have proposed a systematic definition of boundaries for the HP/system balance. A non-exhaustive list includes the SEPEMO-Build (Zottl et al., 2012) that defines boundaries for the most common HP systems (air, water and ground) and IEA SHC Task 44 (JC. Hadorn and al, 2015) that focuses on combined solar thermal and HP systems boundaries. In the following literature review, diverse system perimeters are taken into account, depending on the author and considered system. SPF_{sys} is therefore used in a generic sense. For detailed information on the boundary balance considered in each study, the reader should refer to the specific reference.

Air and Ground source HP systems

Nowadays, the most common HP systems use air or ground as their heat source (EHPA, 2015, Observ'ER, 2015). Erb et al., 2004, monitor 199 of such systems in Switzerland, both in new and renovated buildings. They observe, in average, an annual system performance factor (SPF_{sys}) of 2.7 for the 105 ASHP, and of 3.5 for the 94 GSHP. Similarly, Miara et al., 2010, monitor 77 HP systems in Germany, the majority with underfloor heating distribution systems. The observed SPF_{sys} is 2.9 for the 18 ASHP and 3.9 for the 56 GSHP. Huchtemann and Müller, 2012 study a subset of latter monitored systems, with a focus on existing single-family houses, that were formerly heated by oil boilers. Of these 43 objects, 21 are ASHP, 17 are GSHP with horizontal heat exchangers, and 5 are GSHP with vertical heat exchangers. The observed SPF_{sys} is, in average, 2.3 for ASHP and 2.9 for GSHP. In comparison, the best systems achieve a SPF_{sys} of 3.0 (air) and 4.0 (ground), which illustrates the high potential of this technology but also the necessity of system optimization.

Besides the aforementioned large-scale benchmarks, comparison of ASHP and GSHP systems is also tackled by simulation studies. For example, Marini, 2013, study the performance of ASHP, GSHP, and groundwater HP (GWHP), in comparison to boiler & split systems, applied respectively for heating and cooling seasons, in a low energy residential building of 15 apartments in northern, central and southern Italy. The results show a primary energy saving of 23% for ASHP, 60% for GSHP and 63% for GWHP (0.187 x 10^{-3} tep/kWh conversion factor of electricity into primary energy).

In rare cases, comparison between ASHP and GSHP is achieved by monitoring real scale systems. Safa et al., 2015 present a performance comparison of a variable capacity ASHP and a horizontal heat exchanger GSHP, both installed side-by-side in twin houses in Canada. For the ASHP, the achieved COP ranges from 1.79 to 5.0 for outdoor temperature of –19 °C and 9 °C respectively; for the GSHP from 3.05 to 3.44 for a ground temperature of 2.7 °C and 5.5 °C respectively.

Combined HP and ST systems

In view of increasing the system performance, focus has lately been set on combining HP and ST collectors. Solar thermal HP systems (SHP) are composed of at least a solar collector field and a HP, but they can also include other heat sources (most commonly air or ground), storages or other components. Furthermore, they can be used for space heating (SH), domestic hot water production (DHW), cooling or any combination of the latter. Consequently, their classification can become quite complex (Buker and Riffat, 2016).

SHP systems are closely analysed by the IEA SHC Task 44 (JC. Hadorn and al, 2015). Frank et al., 2010, propose a system classification that focuses on the interaction between the solar collectors and the HP (parallel, series, regeneration). An analysis of the market availability of such SHP systems (Ruschenburg et al., 2013) shows that 61% of the available systems are parallel only, 6% series only and less than 1% regeneration only; the remaining 33% are a combination of the different configurations.

The SPF_{sys} documented in SHP simulation studies vary widely depending on system configurations, sizing, loads and weather conditions (Haller et al., 2014). As an example, for Strasbourg weather conditions, a medium heat demand of a 144 m^2 SFB (Q_{sh} of 6476 kWh/yr, Q_{dhw} of 2076 kWh/yr, defined in JC. Hadorn and al, 2015) and various system configurations and sizing, the SPF_{sys} varies from 3.6 to 5.9 for air + solar HP systems (Carbonell et al., 2014) and from 3.6 to 6.2 for ground + solar HP system (Bertram, 2014). Apart from the SPF_{sys}, another performance indicator that is used by most studies (Bertram, 2014, Carbonell et al., 2013, Carbonell et al., 2014, Lerch et al., 2015, Ochs et al., 2014, Poppi et al., 2016, Winteler et al., 2014) is the electricity consumption of the system. Some studies also report electricity savings of the SHP system when compared to a reference system without solar collectors.

Combined HP and PV systems

Regarding the combination of solar and HP systems, one of the emerging question concerns the competition or synergy between ST and PV.

In this context, Reda et al., 2015 concentrates on the energy assessment of solar technologies, both PV and ST, coupled with a GSHP for MFB in different Italian localities. Through simulation they were able to understand when to use ST and with what purpose (heating or ground regeneration) as well as to quantify the added value of a PV system. Ghafoor and Fracastoro, 2015 address the issue of optimal sizing of multi-purpose ST systems and compare them with a multi-purpose PV-based HP system, both used to cover heating and cooling demand of office buildings. Their simulation results show that steadily decreasing prices have made PV systems more advantageous, even without consideration of public subsidies. Ochs et al., 2014 search for the optimum share of PV and ST in combination with an ASHP or GWHP, for low energy consumption MFB with different SH and DHW demands. The simulation results indicate that, from an energy point of view, small ST systems are generally favourable compared to PV. From an economic point of view, results strongly depend on the development of the PV system costs. They also mention that ST systems have a higher complexity, and that the maintenance effort might be over-proportional, in particular for small systems.

Other authors focus on PV and HP only. Beck et al., 2017 develop a mixed integer linear programing model for the optimal operation, system configuration and sizing of a residential HP system for a SFB in Stuttgart. Fischer et al., 2017 study the influence of different control strategies and boundary conditions on the performance of a variable speed ASHP

in a MFB. Niederhäuser et al., 2015 explore the contribution of PV production to reduce the electricity consumption of a GSHP on a 4 floor office building in Switzerland. The monitoring results indicate that the PV production increases the SPF_{sys} from 5.3 to 6.9. Franco and Fantozzi, 2016 monitor a combined GSHP and PV system on a SFB in Pisa, in order to test its performance and its capacity to maximize PV self-consumption. Finally, Hirvonen et al., 2016 compare PV self-consumption on a SFB in Finland with different heating systems (HP, district heating and direct electric heating).

Impact of HP on the electric grid

The increased use of electricity for HP systems and its key role in decreasing the use of fossil fuels has not passed unnoticed.

Luickx et al., 2008 study the environmental impact of massive HP introduction on greenhouse gas emission in different electricity-generation systems of 4 European countries (Belgium, France, Germany, Netherlands). They show that scenarios introducing direct HP heating along with gas fired combined heat and power plants could generate significant reductions of greenhouse gas emissions, when compared with classic fossil-fuel heating and electric resistance heating.

Several other studies wonder how massive HP introduction could affect the electric grid. Mancarella et al., 2011 tackle the impact of distributed HP on low voltage distribution networks, by using simulated thermal and electric demands. Case studies carried out for typical urban and rural areas in the UK show how the impact of an all-electric future with HP only might be dramatic and call for substantial network reinforcement. In a further study, Navarro-Espinosa and Mancarella, 2014 tackle the subject by using a probabilistic methodology based on Monte Carlo simulations where real electricity and heat profiles are taken as a starting point. Sensitivity studies show that the impact of massive HP penetration could be much more substantial in houses with lower insulation than modern ones, and how the use of gas boilers as auxiliary means (as opposed to electric auxiliary heater) could postpone the need for network reinforcement. They further notice that the problems appear for earlier penetration levels in the ASHP case relative to the GSHP case.

On the other hand, Love et al., 2017 use the records of the electricity consumption of nearly 700 domestic HP installations in Great Britain, recorded every 2 minutes, to create an aggregated load profile. They show that HP electric consumption has two daily peaks and that the HP peak load does not match the electric grid peak load. Nevertheless, a 20% penetration of HP would create a new electric grid peak, and the peak power demand of the grid would increase by 14%.

Finally, Protopapadaki and Saelens, 2017 use probabilistic methods to assess and quantify the impact of HP and PV on the low-voltage distribution grid, as a function of building and district properties. They use the Monte Carlo approach to simulate an assortment of Belgian residential feeders, with varying size, cable type, HP and PV penetration rates, and buildings of different geometry and insulation quality. Amongst other results, they show that high HP penetration rates would yield overloading and voltage stability problems in feeders designed according to current practice, especially in rural areas. This impact is smaller for PV, however for an installed capacity that is not intended to achieve zero-energy balance.

Particularities of multifamily buildings

Out of the preceding studies only 5 concern MFB (Marini, 2013; Ochs et al., 2014; Reda et al., 2015; Fischer et al., 2017 ; Mancarella et al., 2011). Yet, in Switzerland, 55% of the existing building stock is composed of MFB, against 45% for SFB (Schneider et al., 2016), which demonstrates the high development potential of these systems. However, although the market share of HPs in the residential sector grew from nearly zero in the 1990s to about 50% today, only 10% corresponds to MFB (CSD, 2017).

This can be explained by the fact that the implementation of HP systems in MFB is more complex than in SFB (Annex 50, 2017; Rognon et al., 2017), especially because of: i) multiple households, with diluted decision power and related problems of governance; ii) buildings often located in highly dense urban areas, with limited access to renewable heat sources other than air; iii) if not threated carefully, noise emissions can easily become a barrier; iv) higher shares of DHW in overall heat demand and related high temperature, which can affect the HP performance.

As a consequence, the issue of HP systems for MFB is an emerging research field, which still needs specific attention (Annex 50, 2017).

Objectives

Within this context, a recent study concerns a long term in-situ monitoring of a combined parallel/series air + solar HP system implemented on a MFB with very low heat demand situated in Geneva (Fraga et al., 2015), which resulted in a SPF_{sys} of 2.9. In addition, a numerical study allowed to quantify the optimization potential of the specific system, to investigate the sensitivity to SH and DHW demands, in particular concerning the applicability of the concept in the case of building retrofit, as well as to define design guidelines for such systems (Fraga et al., 2017).

The present study, which was developed within a PhD thesis (Fraga, 2017), complements latter work by focusing on a comparative analysis of the potentials and constraints of various HP heat sources (air, geothermal boreholes, lake, river, groundwater and ST), for different MFB types (new, retrofitted and non-retrofitted), representative of Geneva's building stock.

After a characterization of the various studied heat sources and building demands, we present the HP system layouts, numerical model and adopted sizing values. In a further step we consider complementary PV production, taking into account the available roof area. Finally, we discuss the potential impact of massive development of combined HP and PV on the regional electric grid, in terms of annual balance as well as daily peak loads.

2. Heat sources

2.1. Heat source typologies

The HP heat sources analysed in this study are: i) Air; ii) Geothermal (geothermal boreholes); iii) Lake (lake of Geneva, at a depth of 35 m); iv) River (Rhône river, corresponding to the top layer of the lake); v) Groundwater; vi) Solar (ST unglazed collectors as HP heat absorbers).

Of these heat sources, air, geothermal, solar and to some extent groundwater are locally available (Table 1). The others (lake, river, and to some extent groundwater) are regional heat sources, which may not be available at a local building scale. The spatial constraints of the lake and river heat sources, in relation to the territorial distribution of the heat demand, are subject to a specific distribution infrastructure. As an alternative to local exploitation by decentralized HPs, these heat sources could be exploited by a centralised HP connected to a district heating system (not treated in this study).

Table 1

From these heat sources, geothermal and solar are space extensive, i.e. subject to available roof or ground area in the premises of the building. At local building scale, the other ones can be considered as unlimited heat sources. Their sole limitations would be their local availability (existing distribution infrastructure), legislative/normative constraints (e.g noise levels for air HP systems, environmental protection issues for groundwater) or integration constraints in the building (e.g. integration of air HPs on roof tops).

Finally, this study doesn't consider the use of HPs with horizontal ground heat exchangers, trenches, helixes, baskets (which are highly space intensive and inappropriate for MFBs), nor local or regional waste heat.

Note that, from here forward, whenever the term *hydrothermal* is referred, it concerns lake, river and groundwater heat sources.

2.2. Reference year

While standard weather hourly data is readily available for air temperature, wind, and solar irradiation, such is not the case for the hydrothermal heat sources, in particular concerning the temperatures of deep layers of the lake of Geneva and of the Rhône river. We hence use the following data sets, which cover the 2006 – 2015 decade.

Concerning the common meteorological variables (air temperature, solar irradiation, wind velocity), archives of continuous acquisition on urban and peri-urban sites is being provisioned on the web by the University of Geneva, for several decades (Ineichen, 2013). For the lake of Geneva, hourly temperature data of the "Prieuré" fresh water pumping station (pumped water from a depth of 35 m) was handed over by SIG. For the Rhône river, hourly temperature and flow rate data is available from the Swiss Federal Office for the Environment (FOEN, 2015). Concerning groundwater, a study with monitored data (PGG, 2011) shows that the main groundwater areas in Geneva have a temperature between 10 and 15°C, with variations according to depth and season. Due to the lack of hourly data and for simplification purposes, a constant temperature of 13°C was considered in this study.

To define the most representative year of the decade, the following procedure was adopted for each of the 3 sets of temperatures (air, lake, river): i) The sorted hourly temperatures profiles were averaged on an hourly basis, yielding an average sorted hourly temperature profile; ii) For each year of the decade, the actual sorted hourly temperatures profile was compared to the averaged sorted hourly temperatures profile, in terms of the mean square hourly difference.

A statistical analysis shows that 2010 turns out to be the most representative year of the decade (Fraga, 2017). The corresponding hourly profiles, which will be used throughout this study, are presented in Figure 1. Note that the geothermal borehole temperature, as well as the solar collector temperature fed to the HP, are not presented here, as they result from the forthcoming numerical simulation.

Figure 1

Air is the heat source with higher seasonal and daily variability, with a minimum temperature in winter of -5°C and a maximum temperature in summer of 35°C (in 2010). Next is the river (which is equivalent to the superficial layer of the lake), with smaller seasonal and low daily variability. Its minimum and maximum temperatures, in 2010, are 4°C and 26°C. The lake (35m depth) follows with a minor seasonal variability but some peak temperatures between May and November due to lake currents effects (Viquerat, 2012). Its minimum and maximum temperatures are 5°C and 18°C. Finally, by hypothesis, groundwater has a constant temperature of 13°C. Solar irradiance follows the typical northern hemisphere distribution (higher values in summer, lower in winter), with an important daily variability due to clear or cloudy sky.

3. Heat demands / Buildings

In Geneva (urban canton with high population density), 79% of the heated surface of residential buildings concern multifamily buildings, against 21% for single family buildings (Khoury, 2014). It should be noted that, contrary to the single housing sector, in this region the majority of inhabitants of multifamily houses are tenants.

3.1. Building sample

The exploitation of the above heat sources by HP systems will be tested on the same multi-family building sample which was used in Fraga et al., 2017: i) 2 new buildings with identical low SH demand, but differentiated DHW demand; ii) 3 retrofitted buildings, of which one with low SH and the other ones with intermediate SH demand and differentiated SH distribution temperature; iii) 1 non retrofitted building.

The main characteristics of the building sample (with SH demand corresponding to standard weather data) are summarized in Table 2. Note that 4 of the buildings correspond to real case studies situated in Geneva (*New*, *Retrofit best case*, *Retrofit reference*, *No-retrofit*), while the 2 other are combinations thereof, in terms of DHW demand (*New low DHW*) or of SH distribution temperature (*Retrofit intermediate*).

Table 2

Comparison with a benchmark on the SH demand of the MFB stock of Geneva (Khoury, 2014) shows that, except for *No-Retrofit*, all our buildings are in the 1st decile, meaning that they are representative of the best cases in their respective construction periods. *No-retrofit* is in the 3rd quartile, close to the 4th quartile, meaning that it is representative of lower than average building envelope.

Similarly, a comparison with a benchmark on the DHW demand of the MFB stock of Geneva (Quiquerez, 2017) yields the following results: *New* is in the 4th quartile, amongst the highest values, *Retrofit best case* is slightly above the median, and all other cases (which by definition have the same DHW demand) are in the 2nd quartile, closer to the 1st quartile than the median.

3.2. Rescaling of annual and hourly heat demand

In this section, the building demand is rescaled for 2010, the common reference meteorological year chosen for the heat sources. For the rescaling, we consider that: i) DHW demand is independent of the meteorological year and is therefore the same as for standard weather data; ii) SH demand is rescaled according to the ratio between 2010 and standard weather degree days.

The 2010 SH and DHW demands, as well as SH distribution temperatures, are represented in Figure 2 (annual values) for all 6 cases.

Figure 2

Similarly to Fraga et al., 2017, the hourly demand profile is defined as follows : i) For DHW, the hourly profile is given by the monitored data of a typical multifamily building (Zgraggen, 2010). It is adjusted by a multiplication factor, so that the integral of the load corresponds to the annual DHW demand of the building under consideration; ii) For SH, the hourly load is given by a linear function of the outdoor temperature, and is defined by a set point above which SH is off and by a nominal heat load at 0°C outdoor temperature. The nominal heat load at 0°C is adjusted so that the integral of the load corresponds to the annual SH demand of the building under consideration and for the considered meteorological year; iii) For SH distribution temperature, it is given by a linear function of the outdoor temperature, adjusted to the building typology (see Table 3, section 4.3). The DHW distribution temperature is considered constant, at 55°C. The limits of this methodology, in particular in terms of load curve, is discussed in detail in Fraga et al., 2017. For the particular case of a HP system on a low-energy building, it was shown that simulation results with the modelled heat demand are very similar to simulation results with the monitored heat demand, at least at aggregated system level.

4. Heat production system

4.1. System layout

The exploitation of the diverse heat sources of section 2 is provided by the following system layouts (Figure 3). For all heat sources except solar (i.e. air, geothermal, hydrothermal) the heat source is attributed unequivocally to the HP. The latter provides DHW by maintaining the upper part of the DHW tank within the 50-55°C range, while SH is fed directly to the distribution circuit, with excess heat stored in a SH tank. Besides electricity for the HP, direct electric heating is used either in case of HP failure or in case of simultaneous SH and DHW when storage discharge is not possible (temperature in both SH and DHW tank below the respective demand temperatures).

For the solar heat source: the ST unglazed collectors can either provide heat directly to the demand (SH or DHW), or serve as the heat source for the HP. In case of direct solar production, DHW is provided by way of a preheating storage tank, while SH is fed directly in the distribution circuit; in case of HP production, DHW is provided by maintaining the upper part of the DHW tank within a 50-55°C range, while SH is fed directly to the distribution circuit, with excess heat stored in a SH tank. Direct electric heating is used either in case of HP failure (solar collectors below the temperature limit of the HP evaporator) or in case of simultaneous SH and DHW demand, when storage discharge is not possible.

For both layouts, the system is operated with the following scheme of priorities. Maintaining the DHW tank above 50°C has priority over SH, which can be assured by storage discharge and eventually by direct electric heating. When the DHW storage is above 50°C, the priorities to cover the SH demand are: 1) direct solar heat production (solar HP system only); 2) storage discharge; 3) activation of the HP, with surplus production used to charge the heat storage; 4) direct electric heating, which is activated in case of HP failure or insufficient capacity. A detailed description of these priorities is given in Fraga, 2017.

Figure 3

4.2. Numerical Model

4.2.1.Solar, air and hydrothermal systems

Except for the geothermal borehole system, the simulation algorithm is implemented in TRNSYS. The components are modelled according to energy balance equations, taking into account the following features (see Fraga et al., 2017 for mathematical formulation and further details).

In the case of all heat sources except solar (i.e. air, lake, river, groundwater), the temperature of the heat source is directly used as an input to the HP, disregarding the temperature drop of possible heat exchangers. In the case of the solar HP, the temperature of the heat source (collector output) is given by the thermal balance of the unglazed solar collectors, taking into account the global solar irradiation on the collector plane and the thermal losses with ambient air, including the wind effect. The characteristics of the unglazed solar collectors are given by the standardized lab test (SPF, 2012). The temperature drop due to the solar heat exchanger is disregarded.

The HP is modelled by an input/output table based on the working temperatures (evaporator input, condenser output), as given by the manufacturer (Fraga, 2017). Linear interpolation between the manufacturer data values is provided by Trnsys Type 42. The working temperature of the evaporator is driven by the heat source and is limited to the HP upper operating limit. The working temperature of the condenser is driven by the heat demand, and is limited to the HP lower operating temperature.

Each of the storage tanks is modelled by way of a one-node model (disregarding stratification effects, which should be negligible, given the relatively small heat storage capacities – see section 4.3 – and associated transit times). As an exception, in the case of the solar HP system the DHW storage is modelled with two distinct nodes: one for the lower layer (solar preheating) and another for the upper layer (maintained at DHW distribution temperature). In all cases, the model further takes into account heat losses to the technical room.

Direct electric heating covers the instantaneous difference between demand and production (unlike in a real system, where the electric rod is usually integrated in the heat storage). Auxiliary electricity for circulation pumps is not taken into account.

At system level, the entire set of equations is resolved explicitly for each operating mode. The appropriate operation mode is selected according to the priorities defined above (section 4.1), in function of the DHW and SH demand (load and temperature) and the available temperatures at the level of heat source and storage. The simulation is performed in a time step of 0.1 hours over a complete year, with simulation outputs given in hourly integrated values.

Simulation results are validated with monitored values of a solar heat pump system (Fraga et al., 2017), at component and system level. The validation shows that, for all the energy flows, the discrepancy between the simulation and monitoring annual values is inferior to 5% of Q_{dem}. The order of magnitude of these discrepancies is similar to the monitoring uncertainties. In conclusion, the model is sufficiently robust to reproduce the various energy flows, at the level of monthly profiles and yearly integrals.

4.2.2.Geothermal borehole system

In the case of the geothermal borehole system, the numerical simulation is performed with Pilesim (version 2.1), a front/end tool for the design of heating and/or cooling systems with multiple boreholes (Pahud, 2007). The tool, which is based on the Trnsys software package, allows for dynamic simulation of the system in hourly time step, over a period of up to 50 years. The computation results include: i) The inlet/outlet temperatures of the borehole field and associated heat load; ii) The HP electric consumption and associated COP for matching of the heat demand; iii) The fraction of uncovered demand, due to limited nominal HP power, or to borehole temperature reaching user defined lower/upper bounds.

At the level of boreholes and soil, the model is based on a detailed algorithm of the heat diffusion phenomena, including interaction between multiple boreholes, diffusion in surrounding soil, thermal link to upper surface conditions and influence of the geothermal gradient. The HP is modelled by a COP that varies in function of the evaporator input and condenser output temperatures, with a constant thermodynamic efficiency.

Note that the system boundaries are given by the heat demand (load and temperature) at HP output, thereby not including the integration of downstream components (in particular storage and distribution circuit). For the sake of our study, and for coherence with the simulation of the other sources, this issue is treated as follows: for a given building (hourly SH and DHW demand), hourly data at condenser output (input to Pilesim) is given by the simulated condenser output of the related groundwater HP system.

The Pilesim model is furthermore parametrized as follows: i) the thermal properties of the soil are supposed uniform along the borehole length (conductivity: 2.5 W/m.K, heat capacity: 2.1 MJ/m^3.K) and the geothermal gradient is set to a standard value of 0.03 K/m; ii) the HP is characterized by: i) a nominal COP of 4.5 at 0°C evaporator input / 35°C condenser output, corresponding to a constant thermodynamic efficiency of around 50%; ii) A constant electricity consumption, sized according to the HP nominal capacity $P_{nom,hp}$ in Table 3.

Simulation results are performed in an hourly time step on a total of 50 consecutive years. In the following analysis, annual system performance figures are given as the average over this period.

4.3. System sizing

When combining the different heat sources and building demands, the sizing of the system components occurs as follows: i) The nominal HP capacity (at 0°C evaporator input / 35°C condenser output for water HP, at 2°C/35°C for air HP) is adjusted so as to match the maximal hourly load of combined SH and DHW demand of Table 2; ii) The SH and DHW storage capacities are proportional to the respective maximal hourly loads: for SH, 150 L/kW; for DHW, 40 L/kW for the upper part of the storage and 50 L/kW for the lower part of the storage (solar HP system only).

Further heat source specific considerations are as follows.

The type of HP depends on the heat source: an air to water HP (air source), or a water to water HP (all other sources). In both cases, the electricity for the HP, which depends on the evaporator inlet and condenser outlet temperatures, is given by the manufacturer fact sheet (section 4.2.1). In the case of the air source, it includes the electricity for de-icing, according to bench tests with standard EN14511, 2011, as well as for the fans and pumps on the cold source. Except for this and for direct electric heating, no other auxiliary electricity is taken into account by the diverse system layouts.

For the solar assisted HP, the unglazed solar collector area is set to 3 m^2 per kW of HP capacity, according to the guidelines established in Fraga et al., 2017. As a consequence of the variation in heat demand and maximal load, the specific solar collector area $A_{sol.0}$ varies between 0.09 and 0.23 m^2 per m^2 heated area.

For the geothermal HP, the borehole length is set to 250 m (typical depth for MF buildings in Switzerland), and the distance between boreholes to 6 m (corresponding to a 36 m^2 footprint per borehole). For each building, the number of boreholes is adjusted by numerical simulation, so that the hourly input – output temperature average of the heat carrier doesn't fall below -1.5°C within 50 years of operation (according to SIA384/6, 2010). As a result, the geothermal footprint $A_{geo.0}$ is in the range of 2.1 – 3.3 m^2 per kW of HP capacity (corresponding to 0.08 – 0.19 m^2 per m^2 heated area), depending on the building heat demand. Note that: i) unlike for solar, the m^2 per kW_{hp} sizing factor is not constant, since the ratio between the perimeter and the footprint of the borehole field declines with a rising number of boreholes; as a consequence, the access to the heat in the vicinity of the borehole field decreases with a rising number of boreholes; ii) these sizing factors were obtained for buildings with a heated surface of 1000 m^2, and are subject to variations for other surfaces; iii) recharging of the ground, and it's effect in the system sizing, are not studied in this work.

For boreholes that use water as a heat carrier, the limitation of an input – output temperature average of the heat carrier above 4.5°C within 50 years of operation leads to two times higher sizing values (0.12 – 0.58 m^2/m^2, i.e. 4.1 – 6.1 m^2 per kW HP, depending of the building). The results of the corresponding scenarios are not discussed in this paper (more information in Fraga, 2017).

No specific sizing values are given for air and hydrothermal HPs heat source because they are not space extensive at a building level (see section 2.1).

Table 3 summarizes the component sizing values, in relation with the building heat demand.

Table 3

4.4. Limited roof and ground area

At building scale, air, lake, river and groundwater can be considered as unlimited heat sources (see section 2.1). However, geothermal and solar are space extensive, i.e. the amount of heat supplied by the heat source to the HP is subject to available roof or ground area in the premises of the building.

In order to take into account this limitation, we consider 2 cases: i) An available roof area of 0.2 m^2 per m^2 heated floor area, corresponding to a "low-rise" multifamily building in Geneva (4 storeys, under hypothesis of an 80% ratio between the available roof area, in m^2, and the storey specific heated area, in m^2 per storey); ii) An available roof area of 0.1 m^2 per m^2 heated floor area, which corresponds to a "high-rise" building in Geneva (8 storeys). An illustration of these 2 cases is in Figure 4.

Figure 4

As a reference, Geneva multifamily buildings have in average 5.8 storeys (+/-2.6 standard deviation), against 4.1 storeys (+/- 1.6) in Switzerland (according to a recently developed geo-dependent heat demand model of the Swiss building stock, Schneider et al., 2016).

For simplification purposes, the available ground area for the boreholes is considered to be equal to the available roof area (0.2 or 0.1 m^2/m^2).

With this limitation, and for each building type, solar and geothermal systems are downsized as follows: i) For the solar HP system, the collector area A_{sol} is defined as the minimum value between: a) the previously defined solar collector area per heated area, without considering surface availability ($A_{sol,0}$, Table 3) and b) the new limited roof area (0.2 m^2/m^2 or 0.1 m^2/m^2); ii) For the geothermal HP system, the ground area A_{geo} is defined as the minimum value between: a) the previously defined geothermal footprint per heated area, without considering surface availability ($A_{geo,0}$, Table 3) and b) the new limited ground area (0.2 m^2/m^2 or 0.1 m^2/m^2).

Consequently, according to a previous study Fraga, 2017, the solar HP power is downsized according to eq. (1),

$$P_{hp} = \frac{A_{sol}}{A_{sol,0}} P_{hp,0} \quad (1)$$

Similarly, according to a personal communication by the author of the Pilesim tool, the geothermal HP is downsized according to eq. (2):

$$P_{hp} = \frac{A_{geo}}{A_{geo,0}} P_{hp,0} \quad (2)$$

The component sizing values, in relation with the building heat demand values, are summarized in Annex A.

As for the storage, the SH and DHW storage capacities are the same as in section 4.3 for they depend on the heat demand, which remains unchanged.

Direct electric heating is assumed to cover all auxiliary heat needs, in particular when the downsized HP is not able to cover 100% of the building heat demand.

4.5. Complementary PV production

In a further step, the benefits of adding photovoltaic panels on the available roof area are studied. In order to do so, and for both previous cases (0.2 and 0.1 roof m^2 per heated m^2), the following is assumed: i) For air, lake, river, ground-water and geothermal HP systems, the available roof area is considered to be fully used for PV production; ii) For the solar HP system, only the area that is not used by the thermal solar collectors is available for PV production; iii) PV production is based on 12 % efficiency applied directly to the global horizontal solar irradiation (Quiquerez et al., 2015, Freitas et al., 2016), which leads to an annual electricity production of 150 kWh per m^2 of PV. Note that: i) for compari-son, a simulation of a 100 m^2 horizontal collector field in Geneva with a specific PV software (PVsyst, 2012) shows that the efficiency has a variation of respectively +/- 0.5% in seasonal values and +/- 1.7% in hourly values; ii) the added production by PV in the building façades is disregarded in this study.

The interaction of the HP and PV systems and their relation with the electric grid are represented in Figure 5.

Figure 5

Electricity production from the PV panels E_{pv} is used in priority in the form of self-consumption E_{self}, to partake in the HP system electricity demand E_{sys} (which includes electricity for the heat pump and for auxiliary direct electric heating).

This self-consumption is calculated by taking into account the daily match between E_{pv} and E_{sys}. The excess PV production E_{inject} is injected in the grid. Similarly, the HP system final electricity consumption not covered by PV is purchased from the grid E_{final}. These electricity flows obey the following relations:

$$E_{self} = MIN\left(E_{sys}, E_{pv}\right)\Big|_{\Delta t=24h} \quad (3)$$

$$E_{final} = E_{sys} - E_{self} \quad (4)$$

$$E_{inject} = E_{pv} - E_{self} \quad (5)$$

$$E_{net} = E_{sys} - E_{pv} = E_{final} - E_{inject} \quad (6)$$

Note that the match between E_{pv} and E_{sys} is calculated on daily production and consumption values. Within this study, we do not calculate the match in hourly time step because: a) For SH, the hourly load model is given by a linear function of the outdoor temperature, which does not properly account for finer day/night or hourly dynamics (see Fraga et al., 2017); b) When upscaling the results at regional level (section 5.4), the sum of hourly load peaks would not represent reality because each building will have different dynamics and the load peaks will not occur at the exact same hour; c) The choice of working with daily integrated values can be justified by the possibility of handling the actual hourly missmatch with thermal and/or electric storage. The importance of hourly mismatch and its effect on storage capacity will be discussed further down.

Finally, the above defined electricity balance only takes into account the electricity consumed by the heating system (HP and auxiliary direct electric heating), but not the appliances. As a matter of fact, we consider the PV panels to be installed in concomitance with the HP system, for the purpose of partial covering the induced electricity consumption. While PV production could in principle also be used for appliances, this turns out relatively difficult in the Swiss context, where the large majority of MFB households (74%) are tenants (OFS, 2018). Contrary to building owners, tenants do not have a legal basis to invest into (and benefitting from) on site PV systems. Nonetheless, as a complement to the HP self-consumption, we will in a second step, analyse to what extent the excess PV production E_{inject} could be used to partially cover a typical load curve of MFB appliances.

5. Results and discussion

5.1. Performance indicators

The simulation results will be discussed in terms of the annual performance factor, at the level of the HP (eq. (7)), of the HP system (eq. (8)) or of the combined HP & PV system (eq.(9)) :

$$SPF_{hp} = \frac{Q_{hp}}{E_{hp}} \quad (7)$$

$$SPF_{sys} = \frac{Q_{dem}}{E_{hp}+E_{dir}} \quad (8)$$

$$SPF_{final} = \frac{Q_{dem}}{E_{final}} \quad (9)$$

As a complement, results will also be discussed in terms of annual electricity at the following levels: a) HP consumption (E_{hp}); b) HP system consumption (E_{sys}), including electric heating but without auxiliary electricity; c) combined HP & PV system consumption (E_{final}), concerning HP system electricity not covered by PV; d) excess PV production injected into the grid (E_{inject}).

Moreover, electricity consumption and production will also be discussed in terms of seasonal dynamic (daily values) and be compared to the regional electricity load curve.

5.2. Intrinsic potential of HP heat sources

This section concerns the intrinsic potential of the various HP heat sources, i.e. disregarding possible limitations related to roof area and/or ground area (systems sized according to section 4.3), and disregarding complementary PV production. Performance is discussed at HP and system level.

HP performance

HP performance is presented in Figure 6 and Figure 7.

Figure 6

Figure 7

As can be seen in Figure 6, groundwater has the highest SPF_{hp} values (4.3 - 4.8, depending on the building heat demand) followed by river (3.9 - 4.5) and lake (3.8 - 4.3). The geothermal borehole performance is slightly lower (3.6 - 4.0), while solar and air are at the bottom, with very similar values (solar: 2.9 - 3.5; air: 3.0 - 3.4). This heat source hierarchy is explained by Figure 7, where SPF_{hp} is shown in function of the heat source temperature (heat weighted annual average temperature at evaporator input). As can be seen, the SPF_{hp} values is strongly correlated with the source temperature. The only exception is air. Despite higher temperatures, air yields SPF_{hp} values very close to solar, because the air/water HP is less performant than the water/water HP (higher electricity consumption due to de-icing cycle and cold source fan). Hence, at HP level, the similar values between solar and air reveals that the use of solar collectors as a heat source for the HP (series connection) does not lead to a significant improvement when compared to air (a simpler and cheaper solution).

When comparing the building types, the highest SPF_{hp} are achieved by buildings with low 30°C SH distribution (*New* and *New low DHW*), followed by buildings with 40°C (*Retrofit best case* and *intermediate*) and 50°C (*Retrofit reference* and *No-retrofit*). For buildings with the same SH distribution temperature, variation in SPF_{hp} is due to different shares of DHW (the higher the share, the lower the SPF_{hp}).

For E_{hp}, comparison between heat sources obviously yields same ordering as for SPF_{hp} (high SPF_{hp} corresponding to low E_{hp}), except for solar. In the case of solar, the collectors can deliver heat either to the HP, or directly to demand and storage. This parallel connection allows to cover an important part of the summer heat demand (DHW). The reduced heat produced by the HP leads to a proportional reduction of E_{hp}. This phenomenon is more important for buildings with a large share of DHW.

Finally, the SPF_{hp} turns out to be more sensitive to the type of heat source, than to the type of building. Inversely, in the case of E_{hp} (which is proportional to the heat demand) we observe a higher sensitivity to the type of building than to the type of heat source.

System performance

System performance is presented in Figure 8.

Figure 8

As far as SPF_{sys} is concerned, we observe the same pattern as for the SPF_{hp}, with slightly inferior values. This is explained by the SPF definitions (equations (7) and (8)), where Q_{dem} corresponds to $Q_{hp} - Q_{st.loss}$, while E_{sys} corresponds to $E_{hp} + E_{dir}$. Solar is the only heat source with a different pattern, due the solar direct heat production in summer. In this regard,

solar SPF_{sys} is among the highest for low energy buildings (highest shares of DHW), but among the lowest for less performant buildings (lower shares of DHW).

Hence, although air and solar yield similar SPF_{hp} values, the use of the solar collectors as a parallel heat source (direct solar heat production) strongly improves the SPF_{sys}. However, simpler independent air HP systems in combination with glazed solar collectors might reach a similar overall performance as solar assisted HP systems (not analysed in this study).

Finally, we observe in all cases that E_{sys} is only very slightly higher than E_{hp} (in the order of a 1 – 5 %), meaning that E_{dir} is barely needed.

Most importantly, even if SPF_{sys} is in most cases between 3.0 and 4.5, with a strong dependence on the heat source, the associated E_{sys} varies widely between the building types, in relation with the heat demand. As a result, E_{sys} is in the range of 9.9 – 14.0 kWh/m^2 for *New low DHW*, but rises up to 29.6 – 42.9 kWh/m^2 for *No-retrofit*.

5.3. Potential of combined HP & PV systems

This section concerns the simulation results of the HP & PV systems, i.e. taking into account limitations related to roof area and/or ground area (section 4.4) as well as the benefits of adding PV to the available roof area (section 4.5). For readability, results are first discussed independently of PV self-consumption, which is introduced in a second step. The figures presented in the text concern the case of the low-rise building, while the corresponding figures for the high-rise building can be found in Fraga, 2017.

Without self-consumption

For a low-rise building, the total electricity consumption (E_{sys}) and electrity production (E_{pv}) of the HP & PV systems are represented in Figure 9, along with the balance between electricity consumption and production (E_{net}) and the HP system performance (SPF_{sys}). The figure can be interpreted as follows: i) Squares (at the top) represent the performance of the HP system SPF_{sys}; ii) Solid bars (positive values) represent the total electricity consumption E_{sys} of the HP system; iii) Faded solid bars (negative values) represent the total electricity production E_{pv} of the PV system; iv) Lozenges represent the annual balance between total electricity consumption and production E_{net}.

Figure 9

As pointed out before (section 4.4) only solar and geothermal values are affected by the limited roof and ground areas. Nonetheless, in the case of the low-rise building, no downsizing is required for geothermal, and for solar only the *No-retrofit* building suffers a very slight decrease of solar area (from 0.21 to 0.20 m^2/m^2). For these reasons, the SPF_{sys} and E_{sys} values of Figure 9 are basically the same as in in Figure 8.

Regarding the PV production, the 0.2 m^2/m^2 available roof area allows for a E_{pv} of 29.7 kWh/m^2 (related to the heated floor area), except for buildings with a solar HP system, in which case the remaining available roof area allows for a PV production of 0 – 18.2 kWh/m^2, depending on the heat demand and associated solar collector area.

All in all, the impact of the PV production on the annual balance of final purchased / injected electricity (E_{net}) is as follows: i) Except for solar HP systems, and in all cases except for *No-retrofit*, the system produces more electricity than it consumes ($E_{pv} \geq E_{sys}$), so that E_{net} is inferior to zero; *No-retrofit* is the only building type with a positive E_{net} ($E_{pv} \leq E_{sys}$); ii) For solar HP systems, only the building with the lowest heat demand *New low DHW* achieves a E_{pv} higher than E_{sys}.

With self consumption

In Figure 10, the same systems are analyzed taking into account the PV self-consumption (daily match between PV production and HP consumption). The figure can be interpreted as follows: i) The squares (top) represent the performance of the HP & PV system SPF_{final}; ii) Hashed bars are the self-consumed electricity E_{self} (daily match between E_{pv} and E_{sys}); iii) Solid bars (positive values) represent the final purchased electricity from the grid E_{final} (difference between E_{sys} and E_{self}); iv) Faded solid bars (negative values) represent the electricity injected into the grid E_{inject} (difference between E_{pv} and E_{self}); v) The dots represent the annual balance between final purchased electricity and electricity injected into the grid E_{net}.

Figure 10

The self-consumed PV production E_{self} amounts in all cases to around 10 kWh/m^2, except for solar HP systems, for which it varies between 0 – 5.3 kWh/m^2 due to limited production. As a notable result, even when E_{pv} compensates for E_{sys} ($E_{net} \leq 0$), E_{final} and E_{inject} can reach important values. As an example, the *Retrofit reference* building with an air source HP is close to a net-zero energy heating system, but E_{final} amounts to 17.0 kWh/m^2/yr and E_{inject} to 18.9 kWh/m^2/yr. This points out the seasonal mismatch between PV production and heat demand.

The final purchased electricity from the grid E_{final} is in the range of 2.1 – 12.1 kWh/m^2 for the three low energy buildings (*New*, *New low DHW*, *Retrofit best case*). For the *No-retrofit* building, it is essentially above 20 kWh/m^2, reaching up to 39.0 kWh/m^2 in the case of solar HP. The *Retrofit intermediate* and *Retrofit reference* buildings are in between, with values below 15 kWh/m^2, except for air and solar HPs.

These E_{final} values lead to fairly high SPF_{final}. In the case of the three low energy buildings, SPF_{final} is always above 5 and, in the case of groundwater, it reaches values of 17.2 for *New*, 21.9 for *New low DHW* and 12.7 for *Retrofit best case*. The *No-retrofit* building has the lowest values (3.2 - 6.5, depending on the heat source), while *Retrofit intermediate* and *Retrofit reference* have intermediate values (4 – 9.7 and 4 – 7.8).

Overall, groundwater has the lowest E_{final} and the highest SPF_{final} values, followed by river, lake, geothermal, air and solar. However, even though the SPF_{final} values may suggest otherwise, this classification is not that relevant for low heat demand buildings, since the associated E_{final} remains quite low (no matter what heat source is chosen), whereas it is a key issue for higher demands due to the high E_{final}.

High-rise building

In the case of the high-rise building (0.1 m^2/m^2), for which corresponding figures are presented in Fraga, 2017, downsizing is noticeable for both geothermal and solar HP systems: i) for the *Retrofit intermediate* building (E_{sys} increase of 6% and 7%); ii) for the *Retrofit reference* building (E_{sys} increase of 11% and 6%); iii) for the *No-retrofit* building (E_{sys} increase of 43% and 25%).

In the case of the solar HP, the 0.1 m^2/m^2 available roof area is completely used for thermal production, so that E_{pv} is null, hence E_{final} is equal to E_{sys}. In all other cases, E_{pv} amounts to 14.8 kWh/m^2 (half the value of the low-rise building). However, the reduction of the PV production has a limited effect on E_{self}, which amounts to around 8 kWh/m^2, and mainly impacts E_{inject}.

In average, E_{final} turns out 27% higher and SPF_{final} 32% lower than for the case of the low-rise building (average values given by linear regression, with R2 coefficients of 0.94 and 0.89, in Annex B).

Hourly versus daily PV-HP match

As a complement, preceding analysis was also conducted on an hourly match between E_{pv} and E_{sys} (Annex C). As well for the low-rise as for the high-rise building, annual self-consumption E_{self} systematically drops to about 50% of the value

calculated in daily match. This discrepancy is in the range of 3.7 – 6.1 kWh per m^2 heated surface for the low-rise buildings (resp. 2.8 – 4.3 kWh per m^2 for the high-rise buildings), except for solar HP systems (for which PV production is low, and hence also the mismatch).

The effect of this discrepancy on E_{final} is relatively high for buildings with a low heat demand (i.e. with E_{final} below 15 kWh/m^2), but remains below 30% (resp. 20%) for buildings with a higher demand. As pointed out before, this discrepancy would diminish in the case of an aggregated building stock, due to non-synchronic demand profiles.

As pointed out above, the hourly mismatch could also be handled by a daily storage. In daily average, the resulting electric storage requisite would amount to 10 – 17 Wh/m^2 (resp. 8 – 12 Wh/m^2). The maximum electric storage capacity (worst daily discrepancy between daily and hourly match) remains in all cases lower than 110 Wh/m^2 (resp. 70 Wh/m^2), which for a 1000 m^2 building corresponds to about 1 m^3 batteries (resp. 0.6 m^3). Note that these values do not take into account possible storage losses, which should however not exceed 15% (Parra et al., 2016).

PV self-consumption for appliances

Finally, we analyse the potential of the excess PV production to partially cover a typical load curve of MFB household appliances. The load curve is generated by the Electrowhat model (Schneider et al., 2017), which decomposes the yearly electricity consumption of a given building sample into hourly load curves per activity and per electric appliance, based on a library of existing load curves. In our case, latter load curve is scaled to an annual integral of 25 kWh per m^2 heated area, which corresponds to the average annual demand for household appliances of 4'234 MFB (55'325 households), as billed by Geneva's utility company. The resulting load curve is compared to the excess PV production E_{inject} of our buildings and HP systems sample.

As a result (Table 4), in the case of the low-rise buildings an average of 60% of E_{inject} could be used on site, covering 46% of the annual demand of the appliances (average values over all building types and HP systems, except for solar HP, for which E_{PV} and hence E_{inject} are drastically reduced). In the case of the high-rise buildings, 93% of E_{inject} could be used on site, covering 27% of the annual demand of the appliances. Similarly to the HP system analysis, preceding results concern the match of daily profiles. When matching hourly profiles, the resulting values obviously turn out lower (Table 4).

Table 4

5.4. Potential effect on regional load curve

In this section, the final purchased / injected electricity of the combined HP & PV systems is analysed in terms of its annual dynamic, in daily values. Results are presented in Figure 11 for Retrofit best case (the least performant low heat demand building) as well as No-retrofit (the least performant heat demand building), both low-rise buildings. Results for all building sample, low-rise and high-rise, can be found in Fraga, 2017.

Figure 11 can be interpreted as follows: i) Positive values represent final electricity purchased from the grid E_{final}, negative values represent electricity injected in the grid E_{inject}; ii) Values in Wh/m^2/day (left axis) indicate the electricity per heated m^2 of the considered building; iii) Values in GWh/day (right axis) indicate the equivalent grid load, assuming that the entire multifamily building stock of Geneva (19.3 million m^2) was: a) composed by buildings with the same given heat demand; b) equipped with combined HP & PV systems with the same heat source.

Figure 11

For comparison, we also show (in black) the total electricity load of the canton of Geneva in GWh/day (daily values given by the sum of real 2010 hourly data, handed over by the local utility company). The annual electricity consumption of the canton is 2988 GWh, with a maximum daily peak load of 9.6 GWh/day. Currently the share of electric heating is low, therefore there is a low seasonal variation in the load curve. The oscillation of the curve is due to weekend (low values) and weekdays (high values).

For low-rise buildings (Figure 11), the daily peak load of purchased electricity is mainly below 150 Wh/m^2/day for low heat demand buildings (*New*, *New low DHW*, *Retrofit best case*). If the entire multifamily building stock of Geneva (19.3 million m^2) was composed of these types of buildings, the daily peak load of purchased electricity would be mainly below 3 GWh, which corresponds to 30% of the canton's electricity daily peak load.

Regarding the extreme opposite case, the *No-retrofit* building, the daily peak load of purchased electricity is always above 250 Wh/m^2/day (which corresponds to an equivalent daily peak load of 4.8 GWh/day, i.e. 50% of the canton's daily peak load).

As can be seen, the seasonal variation in the total electricity load of the canton of Geneva would change significantly with increasing share of heat pumps used for heating in particular of existing (i.e. non-renovated) buildings. This would also imply a variation of the electricity mix (not discussed within this paper).

5.5. Discussion

The performance of the combined HP & PV systems is represented in Figure 12 as a function of the building heat demand (SH + DHW), for the various heat sources. The performance is analysed in terms of the following indicators: i) The final purchased electricity E_{final} expressed in terms of annual value (kWh/m^2/year, left axis) as well as percentage of equivalent grid energy (right axis); ii) The final purchased electricity E_{final} expressed in terms of daily peak load (Wh/m^2/day, left axis) as well as percentage of equivalent grid daily peak load (right axis); iii) The performance factor of the combined HP & PV system (SPF_{final}).

As indicative values, we also present the 10% and 30% levels of equivalent grid energy (annual value) and grid daily peak load (daily value). It should be noted that the equivalent grid values (right axis values) hold the assumption from the previous section, i.e. that the entire multifamily building stock of Geneva is composed by buildings with the same given heat demand and equipped with combined HP & PV systems with the same heat source.

Figure 12

From the figure, the following results are drawn:

For buildings with a SH + DHW heat demand below 80 kWh/m^2 (which represent less than 10% of the heated surface of the MFB stock of the Canton, c.f. Khoury, 2014), the various combinations of HP & PV systems result in a final purchased electricity (E_{final}) predominantly below 15 kWh/m^2. Note that this threshold corresponds to an equivalent grid energy of about 10%. For buildings with a heat demand below 130 kWh/m^2 (which represent 75% of the current building stock), the final purchased electricity remains mostly below 45 kWh/m^2. This threshold corresponds to an equivalent grid energy of about 30%. Disregarding cases with a high share of direct electric heating (high-rise building with solar or geothermal HP) the final purchased electricity essentially remains within the range of 2 – 35 kWh/m^2, depending on the building heat demand and the HP heat source. Note that the preceding values would increase by 3 – 6 kWh/m^2 if hourly instead of daily PV-HP match was considered.

As far as the daily peak load is concerned, we have a totally different picture. In all cases, the daily peak load is above 50 Wh/m^2/day, which corresponds to an equivalent grid daily peak load of 10%, and only best case buildings (< 80 kWh/m^2) have a daily peak load below 150 Wh/m^2/day (equivalent grid daily peak load of 30%). Buildings with higher heat demand have in most cases daily peak loads above 150 Wh/m^2/day. For buildings at the 3rd quartile limit (130

kWh/m^2), the daily peak load reaches up to 500 Wh/m^2/day (equivalent grid daily peak load of 100%), or even higher if direct electric heating has an important share (highrise only). Note that preceding values would remain unchanged (less than 1% difference) if hourly instead of daily PV-HP match was considered, since the peak load occurs at a day with negligible PV production.

These values are subject to variation in function of the HP heat source. As well for the annual electricity as for the daily peak load, we observe a factor 2 between the extremes (groundwater and solar). This variation has an important impact in buildings with high heat demands, but is not so significant in best case buildings. Hence, for such buildings, the decision of which heat source to choose will most likely fall on other factors than the system's energy performance (heat source availability, legal restrictions, investment costs, social acceptability, system integration …).

The exact opposite pattern appears for the SPF_{final}. Enormous variations in function of the HP heat source are observed for best case buildings (between 5.5 and 21.8 for low-rise buildings, between 3.8 and 12.6 for high-rise buildings). These variations are much less important for building heat demands above 80 kWh/m^2.

As a complement, Figure 13 represents the electricity injected into the grid E_{inject} in terms of annual value as well as daily peak load.

Figure 13

For low-rise buildings, the annual electricity injected into the grid (E_{inject}) is in all cases in the range of 15 – 20 kWh/m^2 (equivalent grid energy of 10 - 13%), except for solar HP systems for which the reduced available roof area leads to values in the range of 0 – 15 kWh/m^2 (decreasing values with increasing building heat demand). For high-rise buildings these values are halved, respectively null for solar HP systems. If the excess PV production was used for appliances, these values would drop by 60% (low-rise), respectively 93% (high-rise).

As far as the daily peak load is concerned, for low-rise buildings the values do not exceed 200 Wh/m^2/day (equivalent grid daily peak load below 40%). Again, these values are halved for high-rise buildings. If the excess PV production was used for appliances, these values would drop to about 120 Wh/m^2/day (low-rise), respectively 30 Wh/m^2/day.

6. Conclusions

This article covers a comparative analysis of the potentials and constraints of different heat sources (air, geothermal boreholes, lake, river, groundwater and solar thermal) exploited by heat pump (HP) systems implemented in various types of multifamily buildings (MFB) – new, retrofitted and non-retrofitted – which correspond to real case studies situated in Geneva.

After characterizing the various heat sources and building heat demands, as well as presenting the numerical model and adopted sizing values, we study the intrinsic potential of the various HP heat sources, i.e. disregarding possible limitations related to roof area and/or ground area. The simulation results show that, when considering the HP performance alone, the higher the heat source temperature (HP heat weighted temperature), the higher the SPF_{hp}. Thus, groundwater has the highest SPF_{hp} values (4.3 - 4.8, depending on the building heat demand) followed by river (3.9 - 4.5) and lake (3.8 - 4.3). The geothermal borehole performance is slightly lower (3.6 - 4.0), while solar and air are at the bottom, with very similar values (solar: 2.9 - 3.5; air: 3.0 - 3.4). Note that, despite higher heat source temperature, air has a SPF_{hp} close to solar because of higher electricity consumption due to de-icing and heat source fan.

As far as SPF_{sys} is concerned, we observe the same pattern as for the SPF_{hp}, with slightly inferior values. Solar is the only heat source with a different pattern, due the additional solar direct heat production in summer. Hence, although air

and solar yield similar SPF_{hp} values, the use of the solar collectors as a parallel heat source (with additional direct solar heat production) strongly improves the SPF_{sys}.

In a further step we consider complementary PV production for the HP system, taking into account the available roof area and the matching of profiles in daily values. For buildings with a combined space heating and domestic hot water heat demand up to 80 kWh/m^2, which correspond to current best case buildings (10% of the existing MFB stock in Geneva), combined HP & PV systems should lead to an annual final purchased electricity inferior to 15 kWh/m^2 (with a factor 2 between the heat sources extremes), for an associated daily peak load up to 150 Wh/m^2/day. If the entire MFB stock of the Canton of Geneva (19.3 million m^2) was renovated to current best case buildings and if all would use such HP & PV systems, the total final purchased electricity would remain below 10% of the total Cantonal electricity demand. However, the associated daily peak load could rise up to 30% of the cantonal daily peak load. For a heat demand below 130 kWh/m^2 (which is the case of 75% of the existing MFB stock of the Canton), the various combinations of HP & PV systems mainly result in a final purchased electricity below 45 kWh/m^2. The daily peak load reaches up to 500 Wh/m^2/day, or eventually higher in the case of high-rise buildings.

Aside from the final purchased electricity, the annual electricity injected into the grid is in the order of 15 – 20 kWh/m^2 for low-rise buildings, and half that much for high-rise buildings. As an exception, in the case of solar HP systems, the reduced available roof area for PV leads to significantly lower values. If the excess PV production was used for appliances, these values would drop by 60% (low-rise), respectively 93% (high-rise).

As a complement, preceding analysis is also conducted on an hourly match of PV production and HP demand profiles. As a result, annual self-consumption systematically drops to about 50% of the value calculated in daily match. Such is also the case for additional self-consumption of household appliances.

Lastly, and as pointed out at several system levels (HP, HP system, combined HP & PV), SPF alone is not a sufficient indicator for the characterization of the HP system performance. Since SPF is an intensive indicator, it doesn't reflect the absolute value of the electricity demand, which primarily depends on the building heat demand. In this regard, the SPF turns out to be quite sensitive to the HP heat source, whereas the final purchased electricity is mostly affected by the building heat demand. Furthermore, both SPF and annual electricity demand (system or final purchased) are limited to annual balance considerations. As a complement, an indication of the peak electricity load gives valuable indications of the potential stress on the grid.

As for next steps, we are currently monitoring air HP systems implemented in MFBs in Geneva, which will give us insight on the real in-situ performance of these types of systems. Moreover, in collaboration with the Faculty of Sciences of the University of Lisbon, we have an ongoing study on MFB HP systems for a southern Europe climate.

7. Ackowledgements

This work was funded by Services Industriels de Genève (SIG).

8. References

Beck, T., Kondziella, H., Huard, G., Bruckner, T., 2017, Optimal operation, configuration and sizing of generation and storage technologies for residential heat pump systems in the spotlight of self-consumption of photovoltaic electricity, Appl Energ, 188, 604-619.

Bertram, E., 2014, Solar Assisted Heat Pump Systems with Ground Heat Exchanger – Simulation Studies, Energy Procedia, 48, 505-514.

Buker, M.S., Riffat, S.B., 2016, Solar assisted heat pump systems for low temperature water heating applications: A systematic review, Renew Sust Energ Rev, 55, 399-413.

Carbonell, D., Haller, M.Y., Frank, E., 2013, Potential benefit of combining heat pumps with solar thermal for heating and domestic hot water preparation, in: ISES Solar World Congress, Energy Procedia, Cancún, Mexico, pp. 2656 – 2665.

Carbonell, D., Haller, M.Y., Philippen, D., Frank, E., 2014, Simulations of Combined Solar Thermal and Heat Pump Systems for Domestic Hot Water and Space Heating, in: SHC 2013, International Conference on Solar Heating and Cooling for Buildings and Industry, Energy Procedia, Freiburg, Germany, pp. 524-534.

CSD, I., 2017, Task 1: Market overview - country report for Switzerland, Fribourg, Switzerland, 21.

EHPA, 2015, European Heat Pump Market and Statistics Report 2014, European Heat Pump Agency.

Erb, M., Hubacher, P., Ehrbar, M., 2004, Feldanalyse von Wärmepumpenanlagen FAWA 1996-2003 - Final report, Bern, 100.

Fischer, D., Bernhardt, J., Madani, H., Wittwer, C., 2017, Comparison of control approaches for variable speed air source heat pumps considering time variable electricity prices and PV, Appl Energ, 204, 93-105.

Fraga, C., 2017, Heat pump systems for multifamily buildings: which resource for what demand?, in: Faculté de Sciences, University of Geneva, Geneva, pp. 143.

Fraga, C., Hollmuller, P., Mermoud, F., Lachal, B., 2017, Solar assisted heat pump system for multifamily buildings: Towards a seasonal performance factor of 5? Numerical sensitivity analysis based on a monitored case study, Solar Energy, 146, 543-564.

Fraga, C., Mermoud, F., Hollmuller, P., Pampaloni, E., Lachal, B., 2015, Large solar driven heat pump system for a multifamily building: Long term in-situ monitoring, Solar Energy, 114, 427-439.

Franco, A., Fantozzi, F., 2016, Experimental analysis of a self consumption strategy for residential building: The integration of PV system and geothermal heat pump, Renew Energ, 86, 1075-1085.

Frank, E., Haller, M.Y., Herkel, S., Ruschenburg, J., 2010, systematic Classification of Combined solar thermal and Heat Pump Systems, in: EUROSUN, Graz, Austria, pp. 8.

Freitas, S., Redweik, P., Catita, C., Brito, M.C., 2016, Potencial solar nas cidades, in: VI Congresso Brasileiro de Energia Solar, Belo Horizonte

Ghafoor, A., Fracastoro, G.V., 2015, Cost-effectiveness of multi-purpose solar thermal systems and comparison with PV-based heat pumps, Solar Energy, 113, 272-280.

Haller, M.Y., Carbonell, D., Mojic, I., Winteler, C., Bertram, E., Bunea, M., Lerch, W., Ochs, F., 2014, Solar and heat pump systems – summary of simulation results of the iea shc task 44/hpp annex 38, in: 11th IEA Heat Pump Conference, Montréal, Canada, pp. 12.

Hirvonen, J., Kayo, G., Hasan, A., Sirén, K., 2016, Zero energy level and economic potential of small-scale building-integrated PV with different heating systems in Nordic conditions, Appl Energ, 167, 255-269.

Huchtemann, K., Müller, D., 2012, Evaluation of a field test with retrofit heat pumps, Build Environ, 53, 100-106.

Ineichen, P., 2013, Solar radiation resource in Geneva: measurements, modeling, data quality control, format and accessibility, Geneva, 15.

JC. Hadorn, al, e., 2015, Solar and Heat Pump Systems for Residential Buildings, Ernst & Sohn, Germany.

Khoury, J., 2014, Rénovation énergétique des bâtiments résidentiels collectifs: état des lieux, retours d'expérience et potentiels du parc genevois, in: Faculté des sciences, University of Geneva, Geneva, pp. 306.

Lerch, W., Heinz, A., Heimrath, R., 2015, Direct use of solar energy as heat source for a heat pump in comparison to a conventional parallel solar air heat pump system, Energy and Buildings, 100, 34-42.

Love, J., Smith, A.Z.P., Watson, S., Oikonomou, E., Summerfield, A., Gleeson, C., Biddulph, P., Chiu, L.F., Wingfield, J., Martin, C., Stone, A., Lowe, R., 2017, The addition of heat pump electricity load profiles to GB electricity demand: Evidence from a heat pump field trial, Appl Energ, 204, 332-342.

Luickx, P.J., Helsen, L.M., D'haeseleer, W.D., 2008, Influence of massive heat-pump introduction on the electricity-generation mix and the GHG effect: Comparison between Belgium, France, Germany and The Netherlands, Renewable and Sustainable Energy Reviews, 12, 2140-2158.

Mancarella, P., Gan, C.K., Strbac, G., 2011, Evaluation of the impact of electric heat pumps and distributed CHP on LV networks, in: 2011 IEEE Trondheim PowerTech, pp. 1-7.

Marini, D., 2013, Optimization of HVAC systems for distributed generation as a function of different types of heat sources and climatic conditions, Appl Energ, 102, 813-826.

Mermoud, F., Khoury, J., Lachal, B.M., 2012, Suivi énergétique du bâtiment 40-42 de l'avenue du Gros-Chêne à Onex (GE), rénové selon le standard MINERGIE® Aspects techniques et économiques, Geneva, 137.

Miara, M., Danny, G., Kramer, T., Oltersdorf, T., Wapler, J., 2010, Wärmepumpen Effizienz – Messtechnische Untersuchung von Wärmepumpenanlagen zur Analyse und Bewertung der Effizienz im realen Betrieb, pp. 154.

Navarro-Espinosa, A., Mancarella, P., 2014, Probabilistic modeling and assessment of the impact of electric heat pumps on low voltage distribution networks, Appl Energ, 127, 249-266.

Niederhäuser, E.-L., Huguelet, N., Rouge, M., Guiol, P., Orlando, D., 2015, Novel Approach for Heating/Cooling Systems for Buildings Based on Photovoltaic-heat Pump: Concept and Evaluation, Energy Procedia, 70, 480-485.

Observ'ER, 2015, État des énergies renouvelables - Édition 2015, 15ème bilan EurObserv'ER, Volume 15, pp. 210.

Ochs, F., Dermentzis, G., Feist, W., 2014, Minimization of the residual energy demand of multi-storey Passive Houses – energetic and economic analysis of solar thermal and PV in combination with a heat pump, in: SHC 2013, International Conference on Solar Heating and Cooling for Buildings and Industry, Energy Procedia, Freiburg, Germany, pp. 1124 – 1133.

OFS, 2018, Construction et logement 2016, Office fédérale de la statistique, Neuchâtel, 87.

Parra, D., Walker, G.S., Gillott, M., 2016, Are batteries the optimum PV-coupled energy storage for dwellings?Techno-economic comparison with hot water tanks in the UK, Energy and Buildings, 116, 614-621.

PGG, 2011, Evaluation du potentiel géothermique du canton de Genève (PGG), Volume 1 - Rapport final, Genève, 240.

Poppi, S., Bales, C., Haller, M.Y., Heinz, A., 2016, Influence of boundary conditions and component size on electricity demand in solar thermal and heat pump combisystems, Applied Energy,, 162, 1062-1073.

Protopapadaki, C., Saelens, D., 2017, Heat pump and PV impact on residential low-voltage distribution grids as a function of building and district properties, Appl Energ, 192, 268-281.

Quiquerez, L., 2017, Analyse comparative des consommations de chaleur pour la production d'eau chaude sanitaire estimées à partir de relevés mensuels. Etude sur un échantillon de bâtiments résidentiels collectifs alimentés par un réseau de chaleur à Genève, Genève, 13.

Quiquerez, L., Faessler, J., Lachal, B.M., Mermoud, F., Hollmuller, P., 2015, GIS methodology and case study regarding assessment of the solar potential at territorial level: PV or thermal?, International Journal of Sustainable Energy Planning and Management, 6, 3-16.

Reda, F., Arcuri, N., Loiacono, P., Mazzeo, D., 2015, Energy assessment of solar technologies coupled with a ground source heat pump system for residential energy supply in Southern European climates, Energy, 91, 294-305.

Rognon, F., Yushchenko, A., Rüetschi, M., 2017, Retrofitting fossil-based heating systems with air to water heat pumps in multifamily houses, in: 12th IEA Heat Pump Conference 2017, Rotterdam, pp. 11.

Ruschenburg, J., Herkel, S., Henning, H.M., 2013, A statistical analysis on market-available solar thermal heat pump systems, Solar Energy, 95, 79-89.

Safa, A.A., Fung, A.S., Kumar, R., 2015, Comparative thermal performances of a ground source heat pump and a variable capacity air source heat pump systems for sustainable houses, Applied Thermal Engineering, 81, 279-287.

Schneider, S., Hollmuller, P., Strat, P.L., Khoury, J., Patel, M., Lachal, B., 2017, Spatial–Temporal Analysis of the Heat and Electricity Demand of the Swiss Building Stock, Frontiers in Built Environment, 3.

Schneider, S., Khoury, J., Lachal, B., Hollmuller, P., 2016, Geo-dependent heat demand model of the swiss building stock, in: Sustainable Built Environment (SBE) regional conference, Zurich, pp. 6.

Tornare, G., Barras, G., Elio, R., Baud, F., Scheider, J., Thiele, W., Graf, O., Hollmuller, P., de Oliveira, F., Fell, M., Ledon, S., 2016, Rapport technique et de communication du projet d'assainissement Minergie-P des immeubles « La Cigale » (GE) – Chauffage par pompes à chaleur solaires couplées à des stocks à changement de phase, CH-3003 Berne, 78.

Viquerat, P.-A., 2012, Utilisation des réseaux d'eau lacustre profonde pour la climatisation et le chauffage des bâtiments; bilan énergétique et impacts environnementaux: Etude de cas: le projet GLN (Genève-Lac-Nations) à Genève., in: Faculté des sciences, institut des sciences de l'environnement, institut forel, University of Geneva, Geneva, pp. 268.

Winteler, C., Dott, R., Afjei, T., Hafner, B., 2014, Seasonal Performance of a Combined Solar, Heat Pump and Latent Heat Storage System, in: SHC 2013, International Conference on Solar Heating and Cooling for Buildings and Industry, Energy Procedia, Freiburg, Germany, pp. 689-700.

Zgraggen, J.-M., 2010, Bâtiments résidentiels locatifs à haute performance énergétique : objectifs et réalités, in: Faculté des sciences, University of Geneva, Geneva, pp. 177.

Zottl, A., Nordman, R., Coevoet, M., Riviere, P., Miara, M., Benou, A., Riederer, P., 2012, SEPEMO-Build Project: Concept for evaluation of SPF - A defined methodology for calculation of the seasonal performance factor and a definition which devices of the system have to be included in this calculation. Heat pumps with hydronic heating systems, 18.

Uncategorized References

Annex 50, 2017, Heat Pumps in Multi-Family Buildings for space heating and DHW, 9/11/2017, http://heatpumpingtechnologies.org/annex50/

EN14511, 2011, Air conditioners, liquid chilling packages and heat pumps with electrically driven compressors for space heating and cooling, in: EN14511:2011, European committee for standardization Brussels.

FOEN, 2015, Water: Monitoring data and statistics, 12.2015, http://www.bafu.admin.ch/wasser/index.html?lang=en.

Pahud, D., 2007, PILESIM2, Simulation Tool for Heating/Cooling Systems with Energy Piles or multiple Borehole Heat Exchangers, User Manual, in, Scuola Universitaria Professionale della Svizzera Italiana, Lugano, pp. 50.

PVsyst, 2012, PVsyst, 16.03.2018, http://www.pvsyst.com/en/

SIA384/6, 2010, Sondes géothermiques, in: 384/6, Société suisse des ingénieurs et des architectes, Zurich, pp. 76.

SPF, 2012, Solar Collector Factsheet C1209: Energie Solaire Kollektor AS, 04.07.2016, http://www.solarenergy.ch/fileadmin/daten/reportInterface/kollektoren/factsheets/scf1209fr.pdf

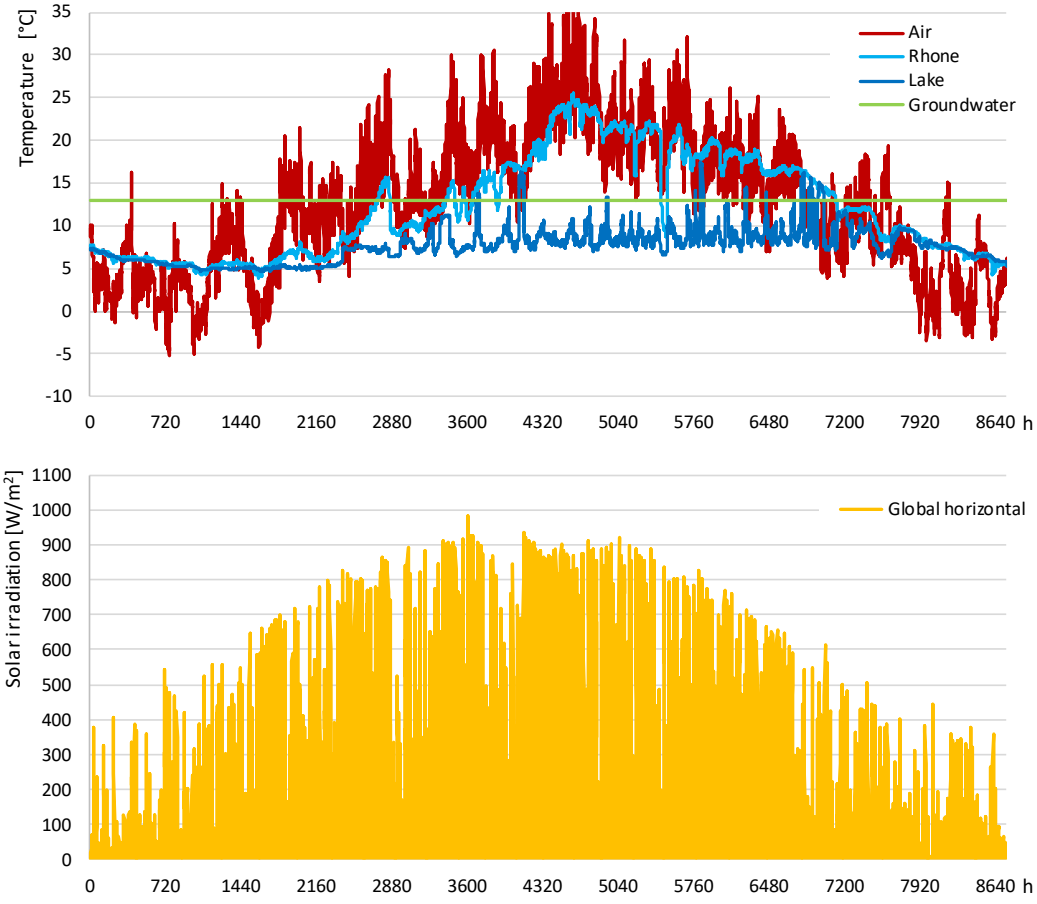

Figure 1 Dynamic profile of air and hydrothermal temperatures (top) and global horizontal solar irradiation (bottom), hourly values (2010).

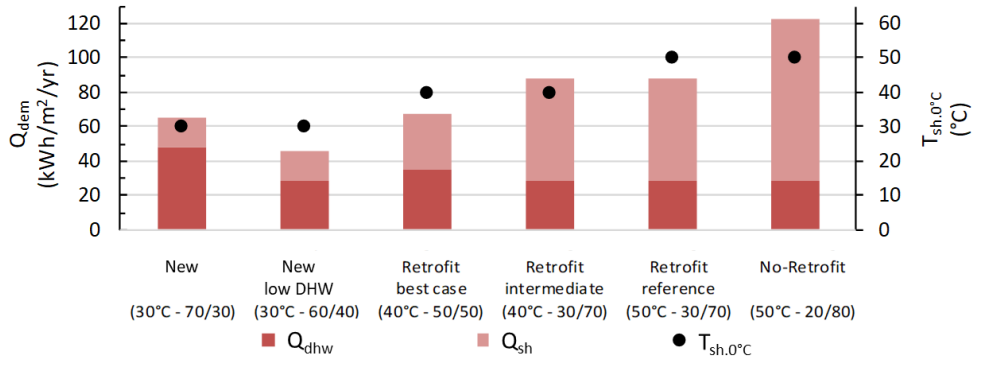

Figure 2 Space heating (SH) and domestic hot water (DHW) demand of the building sample (adjusted to 2010 weather data) as well as SH distribution temperature at 0°C outdoor temperature (dots, right axis).

Air/ geothermal/ hydrothermal HP systems:

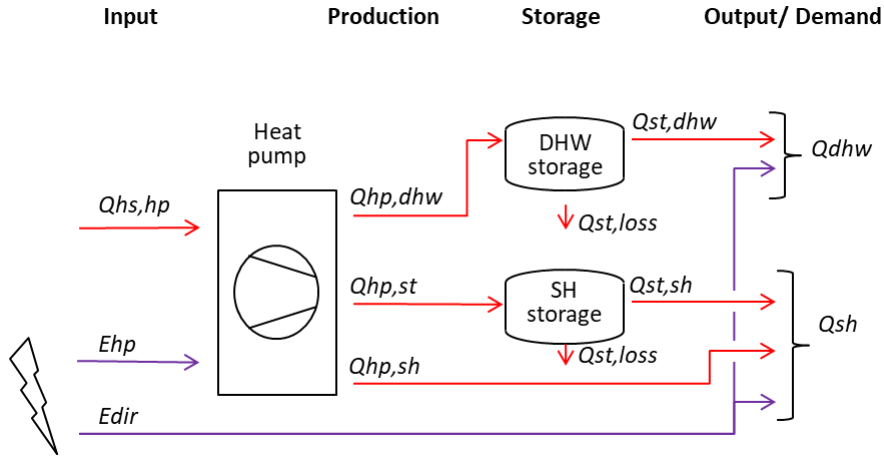

Solar HP system:

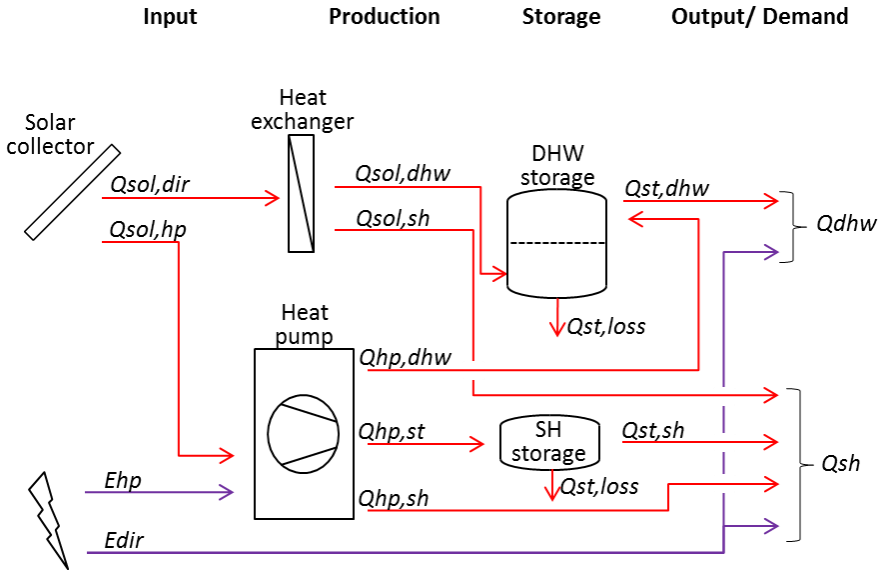

Figure 3 System layout and associated energy flows. Top: with air/ geothermal/ hydrothermal heat sources; Bottom: with solar heat source.

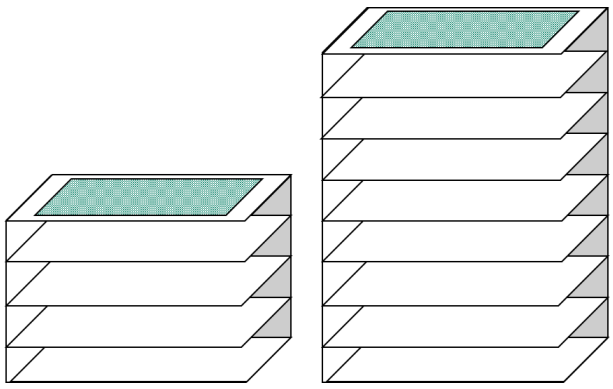

Figure 4 Left - Low-rise Building (0.2 m^2_{roof}/m^2_{SRE}, 4 storeys*); Right - High-rise Building (0.1 m^2_{roof}/m^2_{SRE}, 8 storeys*)
*- Hypothesis of an available roof area (shaded area) equal to 80% of the heated area of a floor.

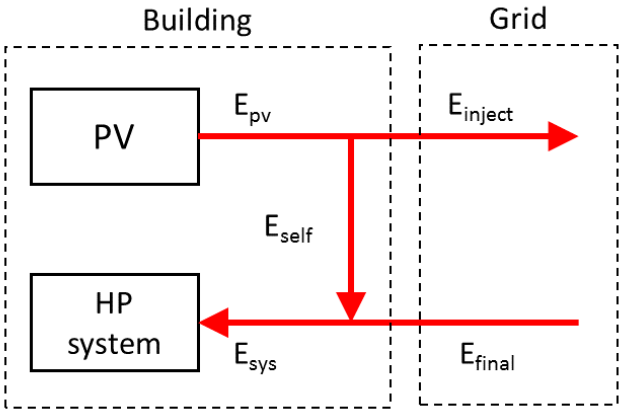

Figure 5 Simplified diagram of HP and PV system's electricity flows.

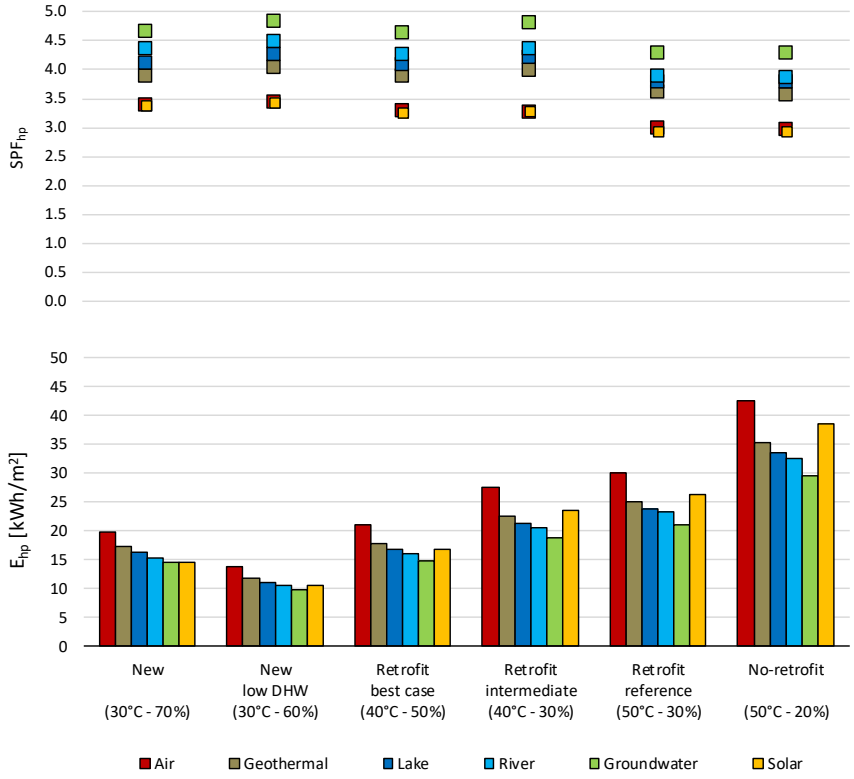

Figure 6 HP performance, sensitivity to building heat demand and heat source (in parentheses: SH distribution temperature – DHW ratio).

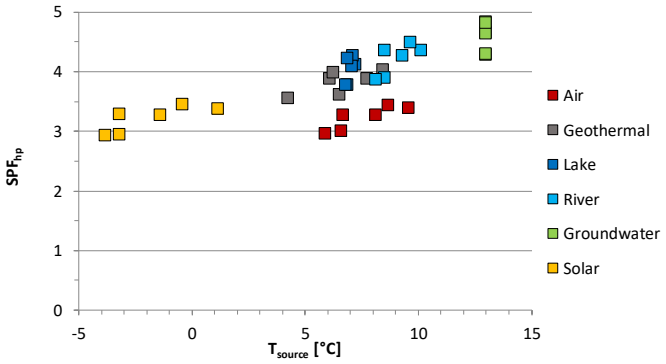

Figure 7 *SPF$_{hp}$* , sensitivity to heat source temperature (heat weighted annual average temperature).

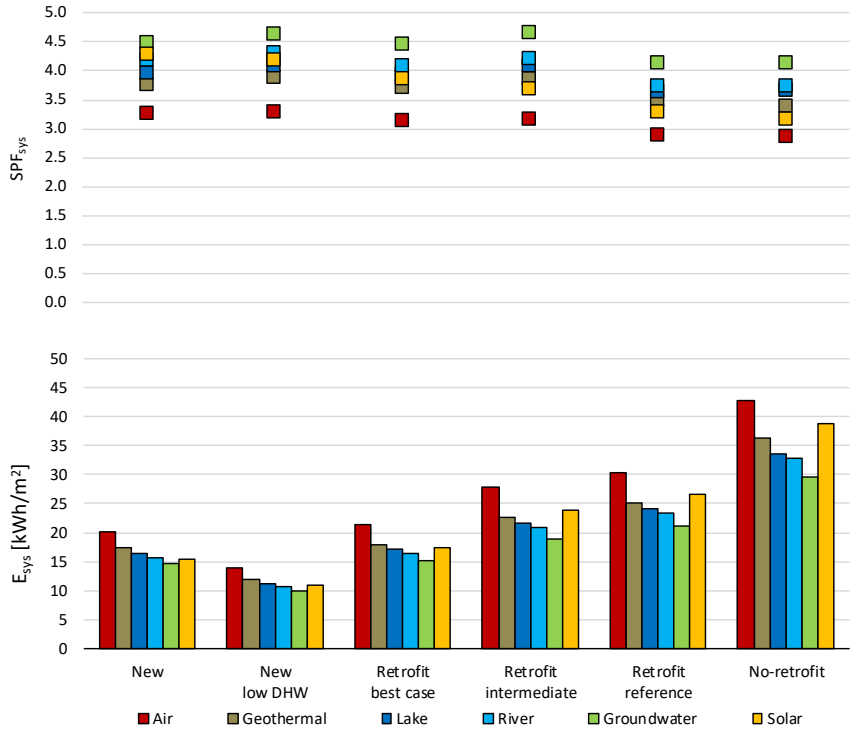

Figure 8 System performance, sensitivity to building heat demand and heat source.

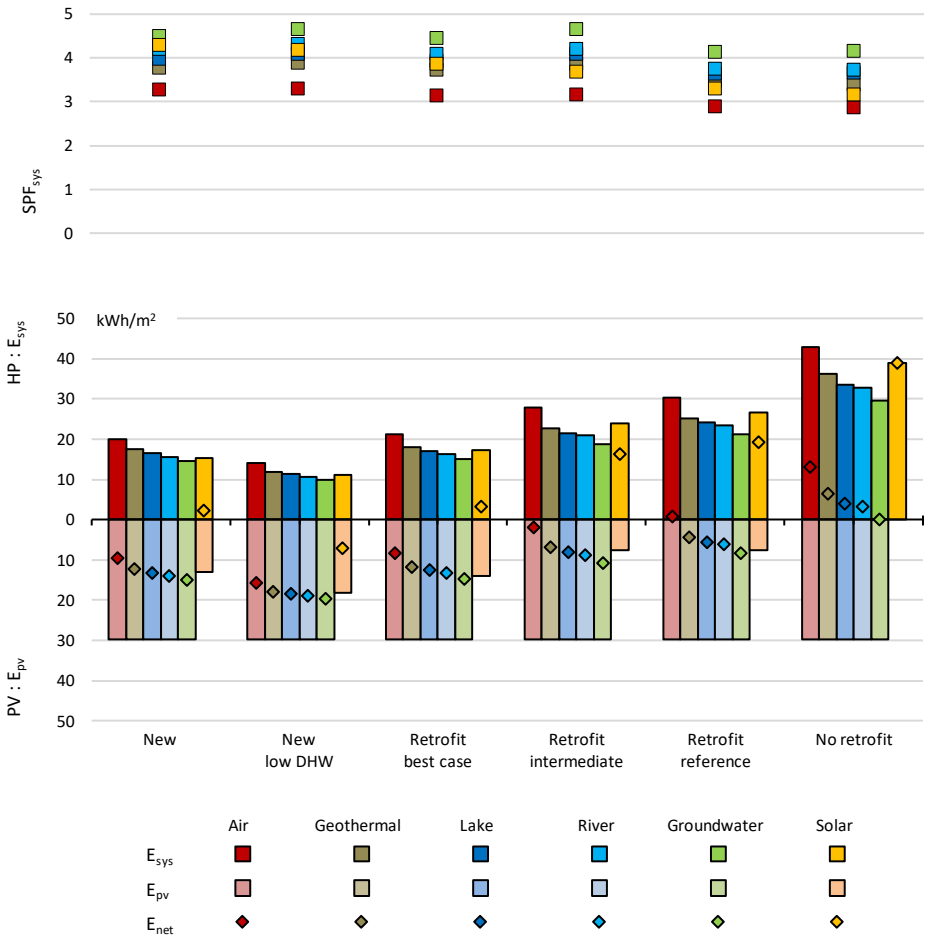

Figure 9 System performance (SPF_{sys}, E_{sys}, E_{pv} and E_{net}) of a HP and PV system in a low-rise building (limited roof/ground area of 0.2 m² per m² of heated area).

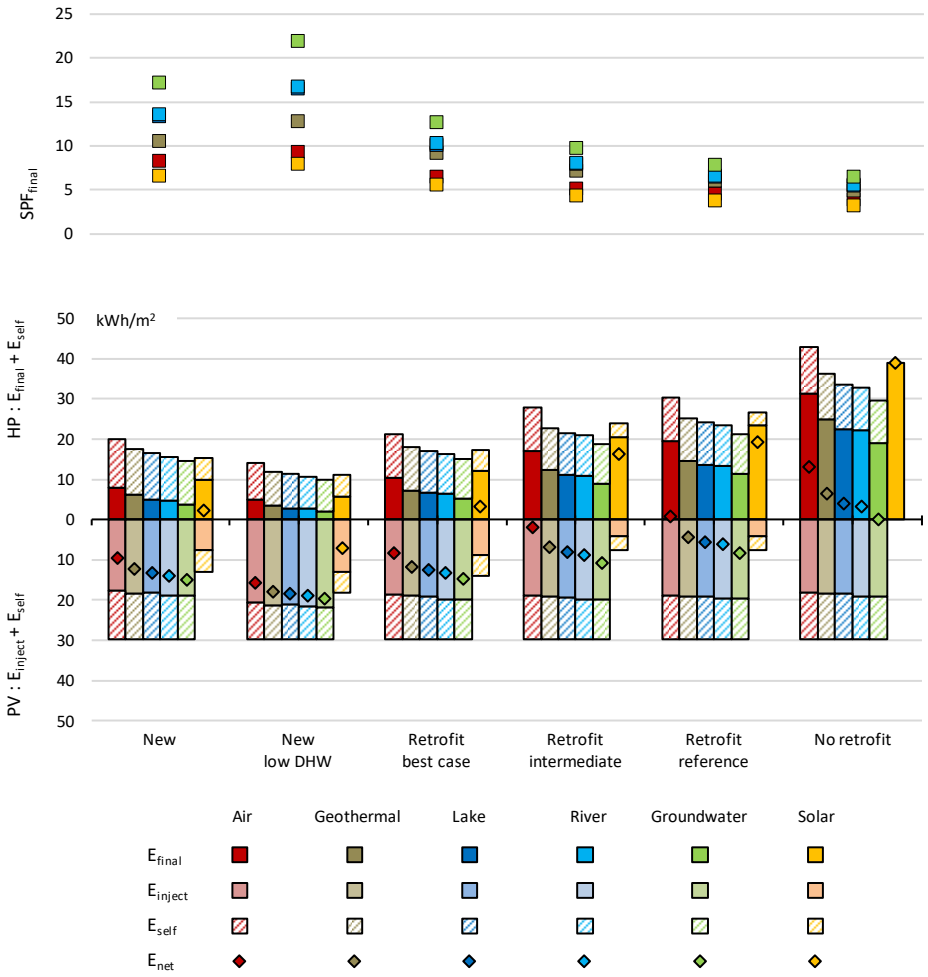

Figure 10 System performance (*SPF*$_{final}$, *E*$_{final}$, *E*$_{inject}$, *E*$_{self}$ and *E*$_{net}$) of a HP and PV system in a low-rise building (limited roof/ground area of 0.2 m² per m² of heated area).

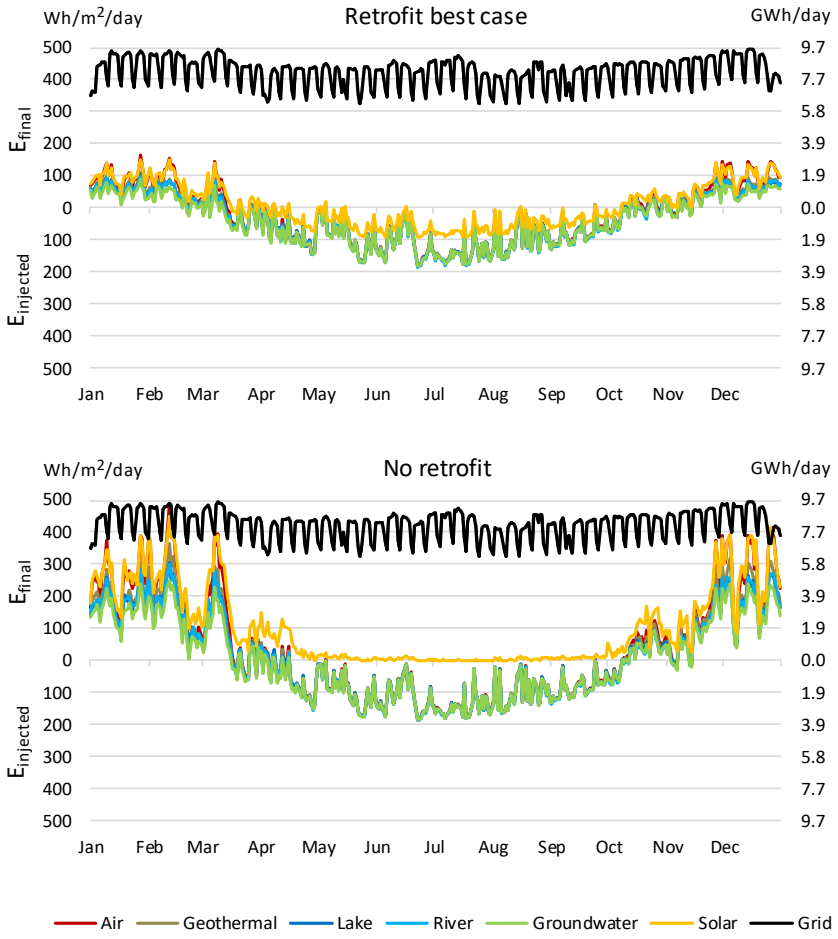

Figure 11 Final purchased E_{final} and injected E_{inject} electricity by the HP and PV systems, in daily values, for a low-rise building (0.2 m^2/m^2). Top: *Retrofit best case*; Bottom: *No retrofit*. The canton of Geneva load curve is represented in black.

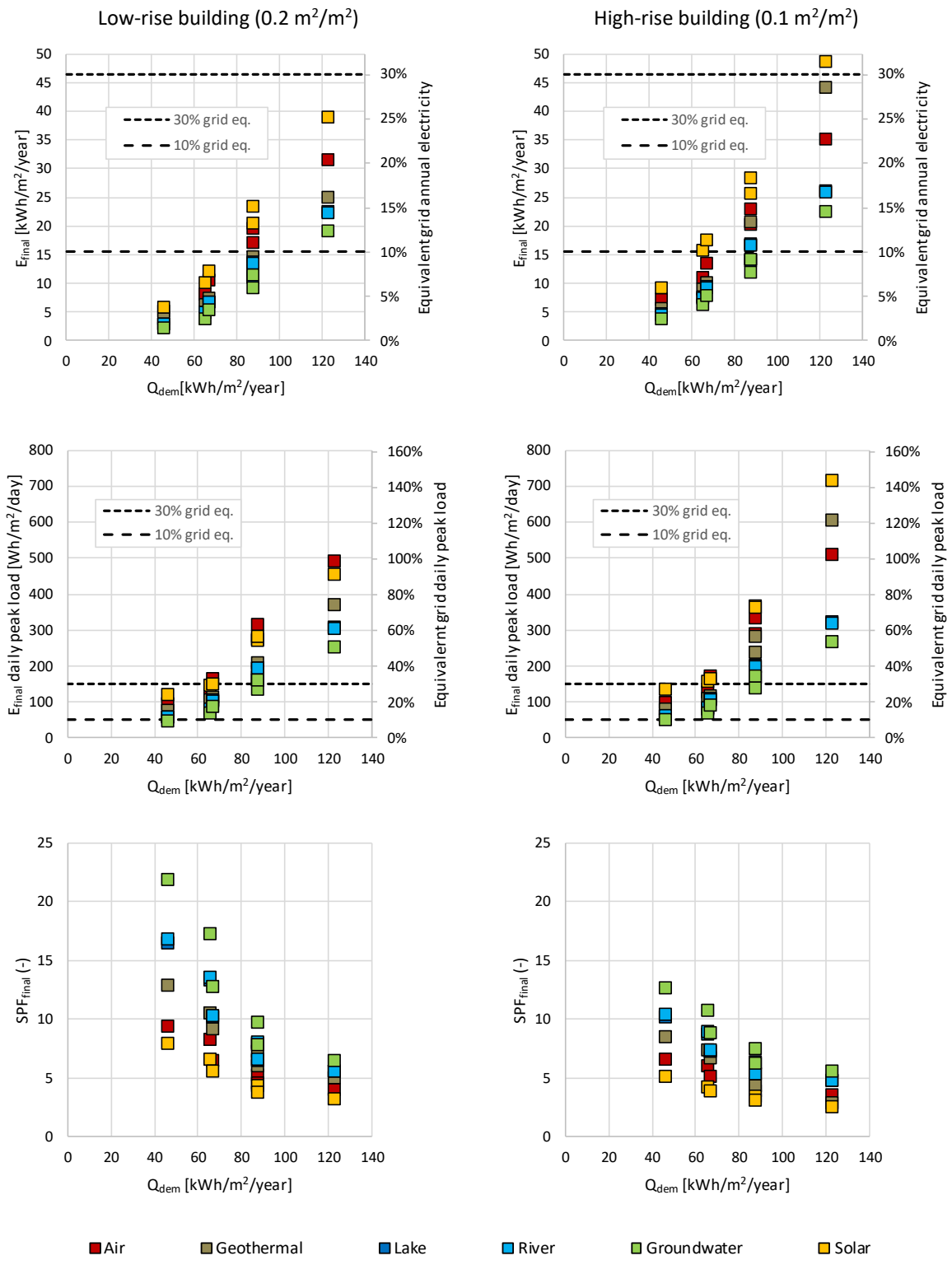

Figure 12 System performance (E_{final} in annual energy and daily peak load, and SPF_{final}) of the combined HP & PV systems, for a low-rise (left) and high-rise (right) buildings.

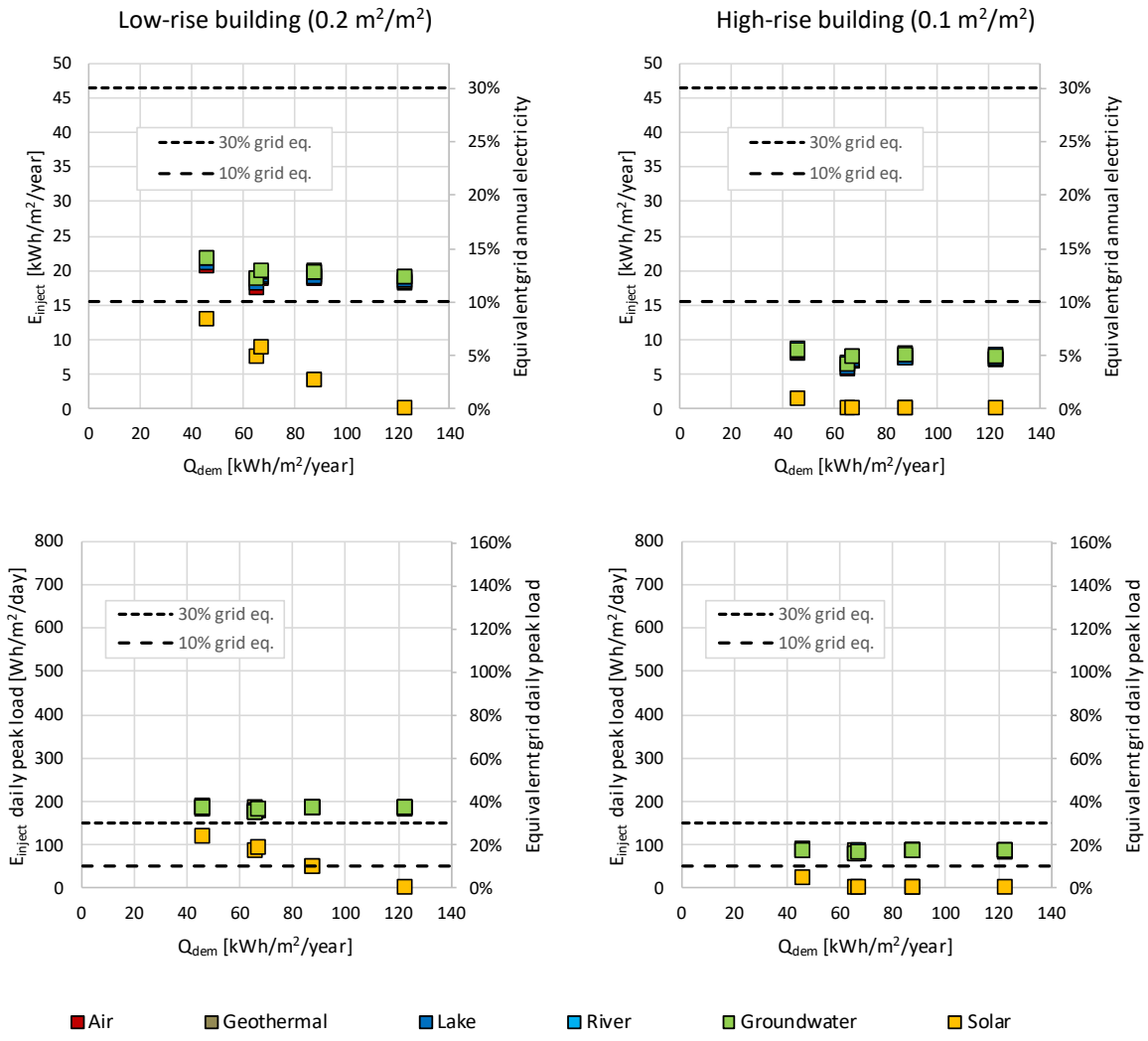

Figure 13 System performance (E_{inject} in annual energy and daily peak load) of the combined HP & PV systems, for a low-rise (left) and high-rise (right) buildings.

	Air	Geo.	Lake	River	Gr. water	Solar
Locally available	x	x			(x)	x
Space extensive		x				x

Table 1 Availability (local or regional) and heat source type (extensive or intensive).

Accronym	Case study	Q_{sh} kWh/m^2	Q_{dhw} kWh/m^2	Q_{dem} kWh/m^2	$T_{sh.0}$ °C
New	(1) SolarCity	20.8	47.7	68.5	30
New low DHW	(1') SolarCity, adapted	20.8	28.3	49.1	30
Retrofit best case	(2) Cigale	37.8	34.6	72.4	40
Retrofit intermediate	(3') Gros Chêne, adapted	69.3	28.3	97.6	40
Retrofit reference	(3) Gros Chêne, build. A	69.3	28.3	97.6	50
No-retrofit	(4) Gros Chêne, build. B	110.0	28.3	138.3	50

Q_{dhw}, Q_{sh}, Q_{dem}: DHW, SH and total annual heat demand (with climatic correction to standard weather).

$T_{sh.0}$: SH distribution temperature, at 0° outdoor temperature.

Case studies: (1) SolarCity (Fraga et al., 2015); (2) Cigale (Tornare et al., 2016); (3-4) Gros-Chêne, building A and B (Mermoud et al., 2012).

Table 2 Main characteristics of the building sample (with climatic correction of SH demand to standard weather data).

			New	*New low DHW*	*Retrofit best case*	*Retrofit intermediate*	*Retrofit reference*	*No-retrofit*
Heat demand	Q_{dhw}	kWh/m^2	47.7	28.3	34.6	28.3	28.3	28.3
	Q_{sh}	kWh /m^2	17.8	17.8	32.5	59.5	59.5	94.4
	Q_{dem}	kWh /m^2	65.5	46.1	67.1	87.8	87.8	122.7
	$P_{max.dhw}$	W/m^2	31.4	18.6	22.8	18.6	18.6	18.6
	$P_{max.sh}$	W/m^2	9.3	9.3	15.0	27.4	27.4	43.6
	$P_{max.dem}$	W/m^2	38.6	25.8	34.9	41.8	41.8	55.9
	$P_{nom.sh.0°C}$	W/m^2	6.9	6.9	11.4	20.9	20.9	33.2
	$T_{sh.off}$	°C	15	15	17	17	17	17
Heat distribution	$T_{sh.0°C}$	°C	30	30	40	40	50	50
	$T_{sh.15°C}$	°C	28	28	30	30	30	30
Storage	St_{hp}	L/m^2	1.29	0.77	0.94	0.77	0.77	0.77
	St_{sh}	L/m^2	1.62	1.62	2.64	5.00	5.00	7.93
	St_{sol}	L/m^2	1.62	0.96	1.17	0.96	0.96	0.96
HP	$P_{nom,hp}$	W/m^2	37.6	25.8	35.0	49.8	49.8	69.8
Solar	$A_{sol.0}$	m^2/m^2	0.113	0.077	0.105	0.149	0.149	0.209
Geothermal	$A_{geo.0}$	m^2/m^2	0.078	0.078	0.117	0.155	0.155	0.194

Q_{dhw}, Q_{sh}, Q_{dem}	DHW, SH and total annual heat demand (with climatic correction to 2010 weather)
$P_{max,dhw}$, $P_{max,sh}$, $P_{max,dem}$	DHW, SH and total maximum hourly heat load
$P_{nom,sh.0°C}$	SH nominal heat load, at 0°C outdoor temperature
$T_{sh.off}$	temperature on/off set-point for SH
$T_{sh.0}$	SH distribution temperature, at 0° outdoor temperature
$T_{sh.15°C}$	temperature of SH distribution, at 15°C outdoor temperature
St_{hp}, St_{sh}, St_{sol}	upper DHW, SH and lower DHW (solar HP system only) storage capacity
$P_{nom,hp}$	HP nominal capacity (at 0°C evaporator input / 35 °C condenser output for water HP or 2°C/35°C for air HP)
$A_{sol.0}$	solar collector area per heated area, without considering surface availability
$A_{geo.0}$	geothermal footprint per heated area, without considering surface availability

Note: in the case of solar and geothermal, these values do not take into account the possible mismatch between foot-prints and surface availability of roof or ground.

Table 3 Building heat demand and correspondent sizing of the system components.

			Daily match		Hourly match	
			Low-rise	High-rise	Low-rise	High-rise
$E_{app,pv} / E_{inject}$	[%]	Avg	60	93	34	58
		Min	57	91	33	57
		Max	63	96	35	59
$E_{app,pv} / E_{app}$	[%]	Avg	46	27	33	25
		Min	42	22	31	23
		Max	53	32	35	27

E_{app}: electricity of appliances

$E_{app,pv}$: electricity of appliances covered by excess PV

E_{inject}: excess PV production (not used by the HP system)

Table 4 PV self-consumption for appliances, in daily and hourly match. Average, minimum and maximum values over the building and HP system sample (except solar HP).

Annex A Sizing of system components taking into account the roof/ground area limitation

		Limit* (m^2/m^2)	*New*	*New low DHW*	*Retrofit best case*	*Retrofit intermediate*	*Retrofit reference*	*No-retrofit*
Solar	$P_{nom,hp}$	N/A	37.6	25.8	35.0	49.8	49.8	69.8
	(W/ m^2)	0.2	37.6	25.8	35.0	49.8	49.8	66.8
		0.1	33.3	25.8	33.3	33.3	33.3	33.3
	A_{sol}	N/A	0.113	0.077	0.105	0.149	0.149	0.209
	(m^2/ m^2)	0.2	0.113	0.077	0.105	0.149	0.149	0.200
		0.1	0.100	0.077	0.100	0.100	0.100	0.100
Geothermal	$P_{nom,hp}$	N/A	37.6	25.8	35.0	49.8	49.8	69.8
	(W/ m^2)	0.2	37.6	25.8	35.0	28.5	28.5	24.0
		0.1	24.2	22.2	18.0	14.3	14.3	12.0
	A_{geo}	N/A	0.078	0.078	0.117	0.155	0.155	0.194
	(m^2/m^2)	0.2	0.078	0.078	0.117	0.155	0.155	0.194
		0.1	0.078	0.078	0.100	0.100	0.100	0.100

$P_{nom,hp}$ HP nominal capacity (at 0°C evaporator input / 35 °C condenser output for water HP)

A_{sol} solar collector area, considering roof surface availability

A_{geo} geothermal footprint, considering ground surface availability and a borehole length of 250m

Limit* available roof or ground surface in m^2 per m^2 of heated floor area of the building

Table B1: Sizing of system components for the different building types, taking into account the roof/ground area limitation

Annex B Highrise and lowrise comparison (E_{final} and SPF_{final})

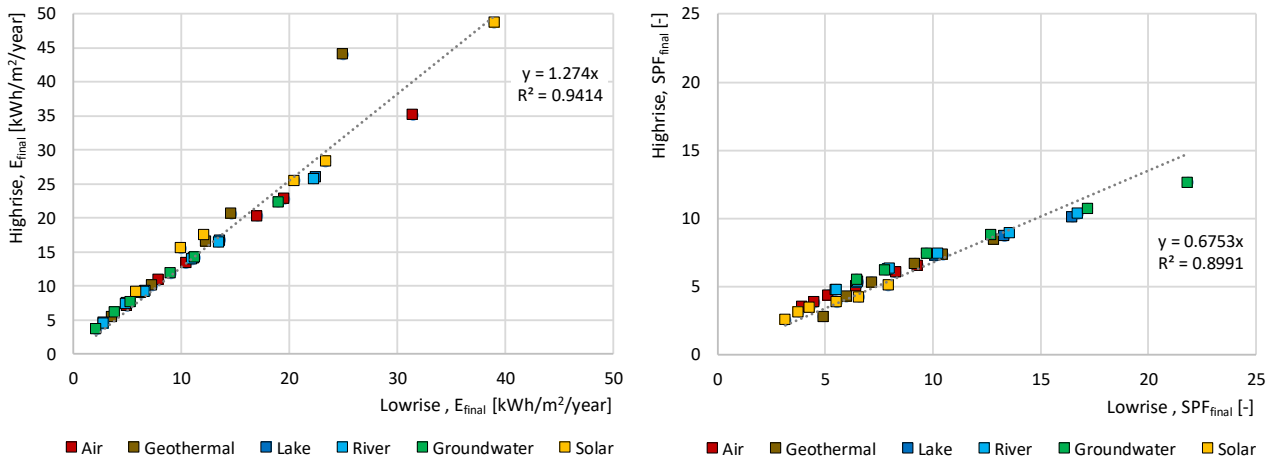

Figure D1: Comparison between highrise and lowrise building results, with respective linear regression, in terms of E_{final} (left) and SPF_{final} (right).

Annex C Hourly versus daily PV-HP match

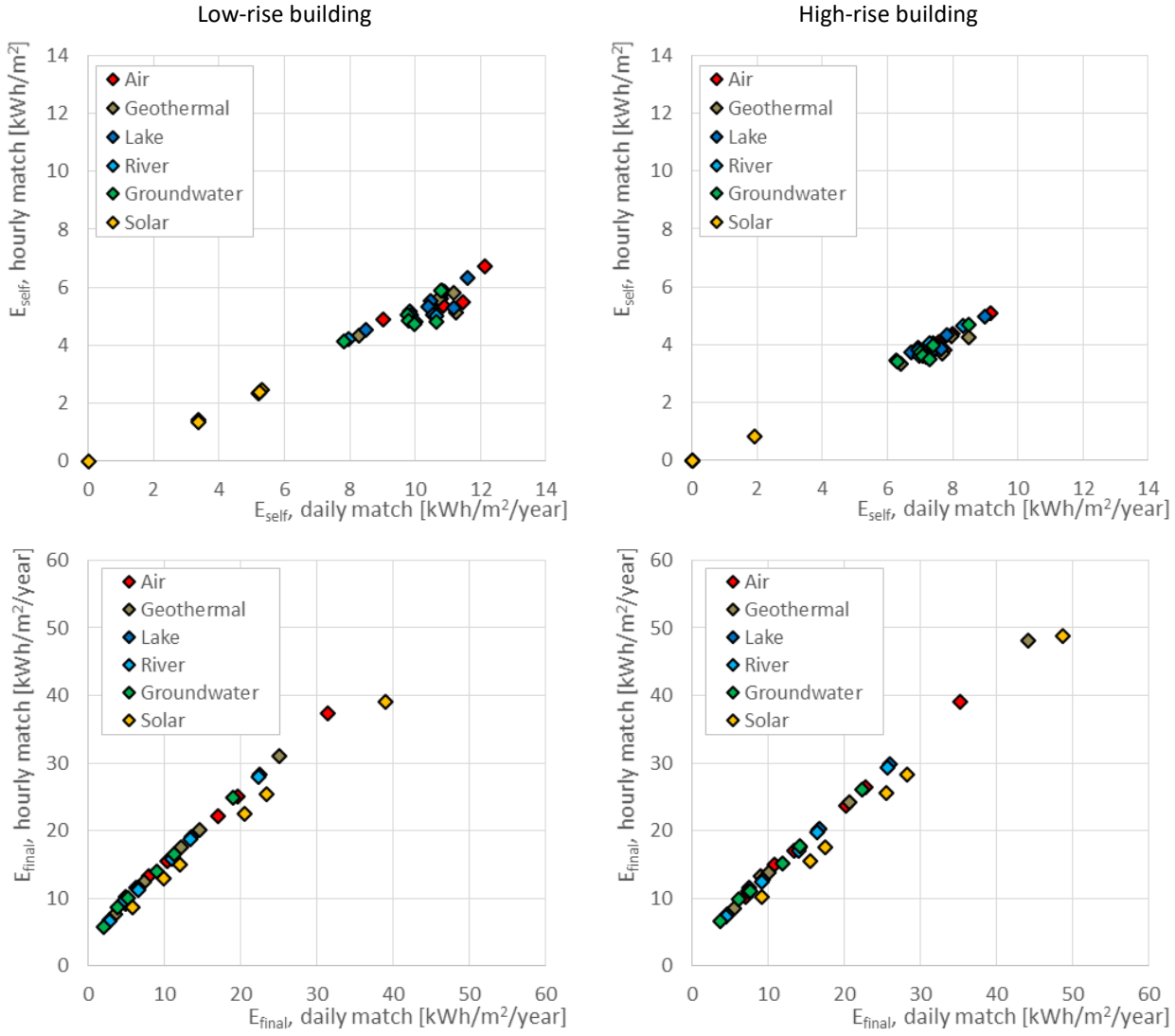

Figure E1: Self-consumption (E_{self}) and purchased electricity (E_{final}), hourly versus daily match.

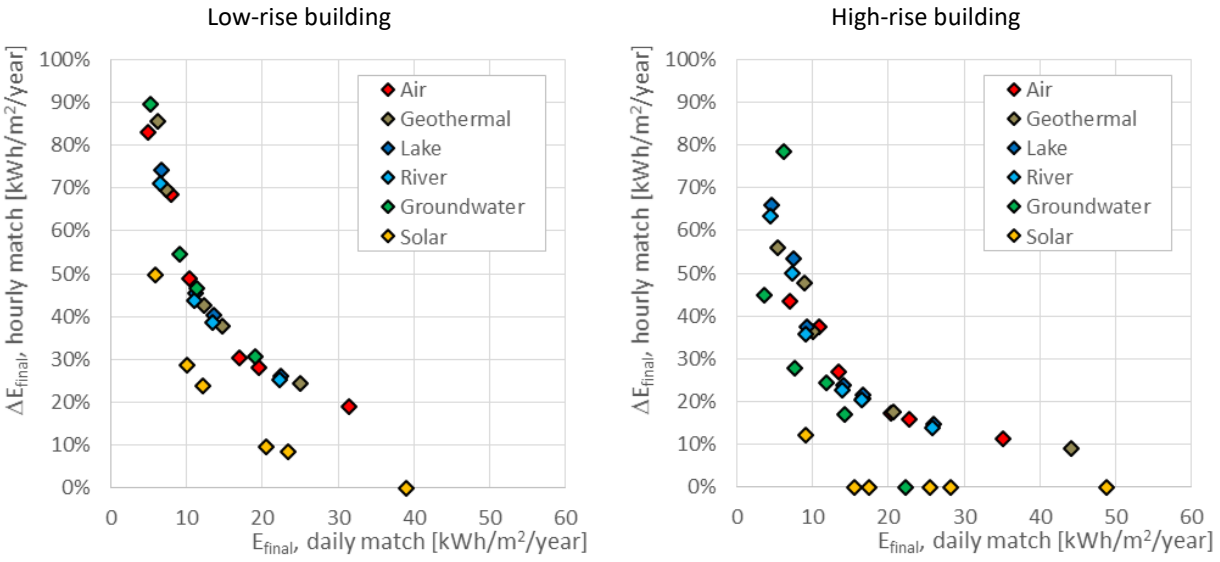

Figure E2: Purchased electricity (E_{final}), relative discrepancy of hourly match versus daily match.

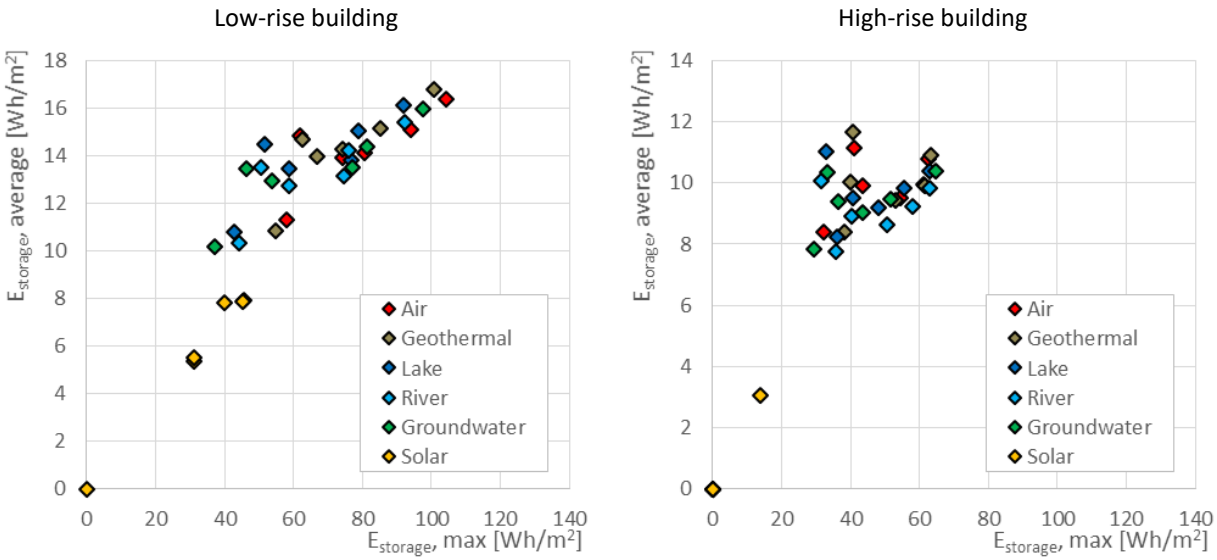

Figure E3: Required daily storage capacity ($E_{storage}$), average versus maximum value.